Bose-Einstein Condensation from a Gluon Transport Equation

Author

Brent Harrison

Supervisor

Prof. Andre Peshier

A thesis presented for the degree of

Masters in Science

Department of Physics

University of Cape Town

February 2018

Declaration of Authorship

I know the meaning of plagiarism and declare that all of the work in this thesis, save for that which is properly acknowledged, is my own.

Signed by candidate | 19/02/2018

Signed | Date

Abstract

In this thesis we investigate the evolution of the quark gluon plasma, as produced in the early stages of a relativistic heavy ion collision, towards equilibrium. To this end we put forward a new numerical scheme to solve the QCD Boltzmann equation in the small-scattering angle approximation, which we develop here for the quenched limit of QCD.

We initially restrict our analysis to spatially homogeneous systems of gluons distributed isotropically in momentum space. With our scheme we confirm results of Blaizot et al. [1], in particular that for certain "overpopulated" initial conditions, a transient Bose-Einstein condensate emerges during equilibriation in a finite time. We further analyse the dynamics of the formation of this condensate.

We then extend our scheme to systems with cylindrically symmetric momentum distributions, in order to investigate the effects of anisotropy. In particular we compare the rates at which isotropization and equilibriation occur. We also compare our results from the small-scattering angle scheme to the relaxation-time approximation.

Acknowledgments

The financial assistance of the National Institute for Theoretical Physics (NITheP) towards this research is hereby acknowledged. Opinions expressed and conclusions arrived at, are those of the author and are not necessarily to be attributed to NITheP.

Many thanks are owed to my supervisor Prof. Andre Peshier for overseeing this project and providing much needed guidance and support. In addition to physics he has taught me the value of taking off my glasses and squinting at equations, and how what appears at first sight to be a free lunch often hides a lurking proverbial devil in the details.

Thank you to Dr. Sylvain Mogliacci for his generous and tireless assistance with all stages of the thesis, from insight into the deeper mysteries of Mathematica to writing the final draft.

I am further indebted to my friends and fellow students Will, Nicole, Greg, Brandon and Charlotte for discussion, collaboration, debugging support, proofreading and various other acts of heroism.

Thank you to my family for helping me stay fed and minimally sleep-deprived.

I would additionally like to express my sincere gratitude to the reviewers for their feedback and the associated time spent working through the details of my thesis. Their comments have been instructive and thought-provoking.

Contents

1 Introduction

1.1 Heavy Ion Collisions and the QGP

The study of quark-gluon plasma (QGP), the phase of strongly interacting matter formed as a result of relativistic nuclear collisions and consisting of quasi-free quarks and gluons, is of increasing relevance in modern physics [2]. It represents a testing ground for the Standard Model, as well as for finite temperature field theory and possible grand unification theories. It is also of cosmological significance, as the early universe was dominated by this phase of matter.

Experiments at the Relativistic Heavy Ion Collider (RHIC) and Large Hadron Collider (LHC) allow us to probe the energy scales at which the QGP may be produced. Inferring its properties and phenomenological behaviour is a central goal of the heavy ion programs at these facilities. The theoretical tools that have been developed to describe it are manifold, as the various stages of a heavy ion collision represent very different physical conditions that demand similarly diverse mathematical formalisms to describe (see figure 1).

Prior to the collision, the nuclei are accelerated to near-light speed, with a Lorentz factor on the order of 100. They are therefore subject to strong Lorentz contraction along the beam axis. At these energies, the lifetime of gluons emitted from the valence quarks or other gluons is long enough to allow additional emissions of soft gluons from themselves. This process keeps increasing the number density of gluons until saturation occurs as recombination of gluons becomes non-negligible, forming the state of matter called the Color Glass Condensate (CGC) [4]. This regime of large gluon number is well approximated by classical dynamics.

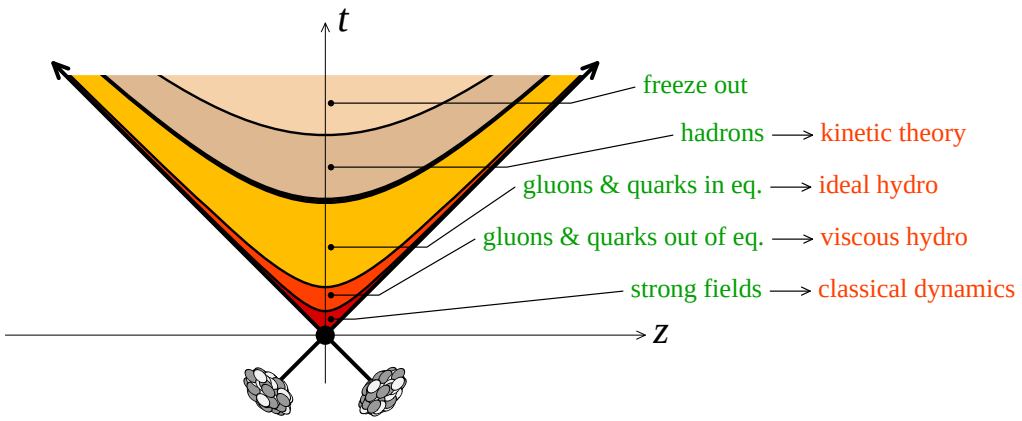

Figure 1: The stages of a heavy ion collision (from [3]).

In the following stage, a large number of gluons are liberated from the CGC. These gluons form a dense, off-equilibrium state called the glasma. Extensive hydrodynamic analyses of HIC indicate that as the medium expands, rapid thermalization occurs (characteristic time on the order of 1 fm) and a QGP in local equilibrium forms. The speed of this thermalization is indicative of strong interactions. As the medium continues to expand and decrease in temperature, it eventually drops below the deconfinement temperature ($T_c \approx 170\,\mathrm{MeV}$) and hadronization occurs.

Using relativistic kinetic theory as an alternative, more fundamental, approach to viscous hydrodynamics, we aim to describe the strong collective behaviour of the QGP from the earliest pre-equilibrium stages through thermalization and eventual freeze-out. To this end we will numerically solve the relativistic Boltzmann equation.

1.2 The Boltzmann Transport Equation

The fundamental equation of kinetic theory is the Boltzmann transport equation. It is a non-linear integro-differential equation governing the evolution of the distribution function of a system of particles in a dilute gas, $f(\boldsymbol{x}, \boldsymbol{p}, t) = dN/dx^3dp^3$, which is the particle number density over phase space.

In the simplest of terms, the Boltzmann equation can be written as

$$D_t f = C[f], \tag{1}$$

where the convective derivative on the LHS $D_t f$ takes into account spatial expansion, i.e. $D_t = \partial_t + \boldsymbol{v} \cdot \boldsymbol{\nabla}$. Here $\boldsymbol{v}$ is the velocity of the particles; in our case (assuming massless gluons) $|\boldsymbol{v}| = 1$. For the purposes of this thesis we will be discussing a spatially uniform distribution of "gluons in a box" and thus will disregard the gradient term. $C[f]$ is called the collision term and encodes the scattering processes that drive the evolution of the system. For binary scattering processes it is given by

$$\begin{aligned} C[f] = \frac{1}{2} \int \frac{d^3p_2}{(2\pi)^2 2E_2} \frac{d^3p_3}{(2\pi)^2 2E_3} \frac{d^3p_4}{(2\pi)^2 2E_4} \frac{1}{2E_1} |\mathcal{M}_{12\to34}|^2 \times \\ \times (2\pi)^4 \delta(p_1 + p_2 - p_3 - p_4)(f_3 f_4 \bar{f}_1 \bar{f}_2 - f_1 f_2 \bar{f}_3 \bar{f}_4). \end{aligned} \tag{2}$$

We will present this term in detail in the next section.

Worth emphasizing is that Eq. (1) with (2) is non-local, non-linear and depends on the six components of position and momentum as well as time.

Exact (analytical) solutions are rare even for less complicated interactions than QCD.

Numerical solutions are in general computationally expensive. In order to make the computation more feasible it is relevant to consider systems with particular symmetries that reduce the degrees of freedom. Additionally, as we will see, more efficient numerical schemes can greatly improve performance.

1.3 The Bose-Einstein Condensate

The Bose-Einstein Condensate (BEC) is a state of matter typically achieved by cooling a dilute gas of bosons to temperatures approaching absolute zero. Under these conditions a large number of bosons occupy the lowest energy state. In mathematical terms, the Bose distribution picks up an additional term in the form of a Dirac delta function at momentum $p = 0$, i.e.

$$f(\boldsymbol{p}) = \frac{1}{e^{p/T} - 1} + (2\pi)^3 n_c \delta(\boldsymbol{p}), \tag{3}$$

where the Dirac delta function is normalized such that

$$\int \frac{d^3p}{(2\pi)^3} (2\pi)^3 n_c \delta(\boldsymbol{p}) = n_c \tag{4}$$

is the number density of the particles in the condensate state.

While the BEC is an established phenomenon in other contexts [5], a condensate of gluons has yet to be empirically observed.

1.4 Thesis Outline

We begin in Sec. 2 with an overview of kinetic theory, in which we will define the distribution function and various thermodynamic quantities that may be derived from it. We then derive the Boltzmann equation for gluons and demonstrate some of its important properties. In particular we will show how the H-theorem proves that closed systems evolving according to it must necessarily converge to a Bose-Einstein distribution.

The ultimate goal of the thesis is to develop and implement an efficient scheme to numerically solve the Boltzmann equation for gluons under the following simplifying assumptions.

We will assume that small angle scatterings dominate, which will allow us to reduce the Boltzmann equation to a Fokker-Planck diffusion equation (described in Sec. 3) that is somewhat easier to solve. We will also assume that $2 \to 2$ processes dominate (at least in some period of time), i.e. that particle number is conserved, and that the distribution function is uniform in space.

We detail the numerical implementation in Sec. 4, including flux-conservative schemes for solving the Fokker-Planck equation under the assumption of spherically and cylindrically symmetric momentum distributions.

In Sec. 5 we present a selection of results. In particular we analyze the evolution of various initial distribution functions to equilibrium. For the spherically symmetric case, we consider both underpopulated and overpopulated systems, the later of which result in the formation of a Bose-Einstein condensate. We compare these results to those obtained using the relaxation time approximation. Generalizing to cylindrical symmetry we investigate the effects of anisotropy in the initial conditions and in particular compare the

rate of thermalization to the rate of isotropization.

Finally, we summarize the project with some comments, conclusions and an outlook for future work. Some useful definitions and details are presented in the Appendices.

2 Relativistic Kinetic Theory

In this section we present the fundamentals of kinetic theory, following [6] and [7].

2.1 Conventions

We will work in natural units ($c = \hbar = k_B = 1$). The choice of Minkowski metric is

$$g^{\mu\nu} = \begin{pmatrix} 1 & 0 & 0 & 0 \\ 0 & -1 & 0 & 0 \\ 0 & 0 & -1 & 0 \\ 0 & 0 & 0 & -1 \end{pmatrix}. \tag{5}$$

For purposes of vector notation, Greek indices will refer to the components of a 4-vector, while Latin indices will denote "spatial" (3D vector) components.

In order to avoid cumbersome notation, we define

$$\int \equiv \frac{1}{(2\pi)^3} \int_{-\infty}^{\infty} \int_{-\infty}^{\infty} \int_{-\infty}^{\infty} dp_x dp_y dp_z. \tag{6}$$

Further, it is understood that the distribution function $f = f(\boldsymbol{x}, \boldsymbol{p}, t)$ is still a function of position, momentum and time even if written without arguments or, e.g. in the case of a spatially homogeneous system simply as $f(\boldsymbol{p}, t)$.

We will frequently write position and momentum four-vectors appearing as

arguments to functions without the indices, i.e. $f(x^\mu) \to f(x)$.

Note that as the only particles we will consider in this thesis are gluons, all mass terms will be set to zero without further comment. Additionally, for notational convenience we will set the gluon degeneracy to 1; $d_g = 16$ can be reinstated as necessary.

2.2 Basic Definitions

In order to describe non-uniform systems of particles, it is necessary to introduce a local number density $n(\boldsymbol{x}, t) = n(x^\mu)$. The number density is defined such that the total number of particles N in a fixed 3-volume element $\Delta^3 x$ is given by

$$N = n(x,t)\Delta^3 x. \tag{7}$$

N is clearly an invariant Lorentz scalar; thus as the volume element is not invariant under Lorentz transformations, neither is n.

Similarly, one defines the local particle current $\boldsymbol{j}(x)$. These quantities n and $\boldsymbol{j}$ can both be expressed in terms of a more general description of the system, the distribution function $f(\boldsymbol{x}, \boldsymbol{p})$. This function gives the distribution of momenta of particles at each space-time point. In particular it is defined such that the number of particles N in a phase-space volume element $\Delta^3 x \Delta^3 p$ around $\boldsymbol{x}, \boldsymbol{p}$ at time t is given by

$$N = f(\boldsymbol{x}, \boldsymbol{p})\Delta^3 x \Delta^3 p. \tag{8}$$

We can now express the density and current (in some specified reference frame) as

$$n(x) = \int \frac{d^3p}{(2\pi)^3} f(x, \boldsymbol{p}) \tag{9}$$

$$\boldsymbol{j}(x) = \int \frac{d^3p}{(2\pi)^3} \boldsymbol{v} f(x, \boldsymbol{p}) \tag{10}$$

where we integrated over all momenta and $\boldsymbol{v} = \boldsymbol{p}/p^0$, where p^0 is the zeroth component of the 4-momentum.

We may combine these expressions, defining the 4-current $N^\mu(x) = (n(x), \boldsymbol{j}(x))$ such that

$$N^\mu(x) = \int \frac{d^3p}{(2\pi)^3} \frac{p^\mu}{p^0} f(x, \boldsymbol{p}), \tag{11}$$

which we recognize as a moment of the distribution function. Now, in order for N^μ to be a 4-vector, the combination $\frac{d^3p}{p^0} f(x, \boldsymbol{p})$ must be a Lorentz scalar. In fact we can easily show that the integration measure $\frac{d^3p}{p^0} = \frac{d^3p}{E}$ is itself Lorentz invariant, and hence $f(x, \boldsymbol{p})$ must be as well.

Without loss of generality, consider a Lorentz boost along the x-axis. The following transformation rules apply.

$$\begin{aligned} E' = \frac{E - p_x v}{\sqrt{1 - v^2}}, \quad p'_x = \frac{p_x - Ev}{\sqrt{1 - v^2}}, \\ p'_y = p_y, \quad p'_z = p_z. \end{aligned} \tag{12}$$

Thus, the phase space element transforms as

$$d^3p' = dp'_x dp_y dp_z = \left(\frac{1}{\sqrt{1-v^2}} - \frac{p_x v}{E\sqrt{1-v^2}} \right) dp_x dp_y dp_z = \frac{E'}{E} d^3p, \quad (13)$$

i.e.

$$\frac{d^3p}{E} = \frac{d^3p'}{E'} \quad (14)$$

as required.

It can similarly be shown [8] that the element $d^3x d^3p$ is a Lorentz invariant, and thus from the definition of the distribution function (8), we can confirm the Lorentz invariance of $f(x, \boldsymbol{p})$.

2.3 The Energy-Momentum Tensor

We continue defining macroscopic quantities of the medium. Consider the energy density. The energy per particle is simply p^0; thus the energy density of the system of particles described by the distribution function f is given by

$$T^{00}(x) = \int \frac{d^3p}{(2\pi)^3} p^0 f(x, \boldsymbol{p}), \quad (15)$$

where the T^{00} notation is chosen in anticipation of the tensor quantity we are about to construct.

Similarly we can define the energy flow T^{0i} by

$$T^{0i}(x) = \int \frac{d^3p}{(2\pi)^3} p^0 v^i f(x, \boldsymbol{p}), \tag{16}$$

(where $v^i = p^i/p^0$) as well as the momentum density,

$$T^{i0}(x) = \int \frac{d^3p}{(2\pi)^3} p^i f(x, \boldsymbol{p}), \tag{17}$$

which obviously agrees with the energy flux component T^{0i}.

Finally we define the momentum flux density or pressure tensor T^{ij}, which is the flow in the direction $\hat{j}$ of the momentum in the direction $\hat{i}$,

$$T^{ij}(x) = \int \frac{d^3p}{(2\pi)^3} p^i v^j f(x, \boldsymbol{p}). \tag{18}$$

We can combine these sixteen quantities (15) - (18) into the covariant form

$$T^{\mu\nu}(x) = \int \frac{d^3p}{(2\pi)^3} \frac{p^\mu p^\nu}{p^0} f(x, \boldsymbol{p}). \tag{19}$$

This is the energy-momentum tensor, which we recognize as a "second moment" of the distribution function. (Similarly the particle 4-current (11) is a "first moment".)

For an ideal fluid the energy-momentum tensor has the form [9]

$$T^{\mu\nu} = (\epsilon + P) u^\mu u^\nu - P g^{\mu\nu}, \tag{20}$$

where ϵ and P are the energy density and pressure, respectively, and u^μ is the four-velocity of the fluid.

2.4 Hydrodynamic Flow

The hydrodynamic flow velocity of a medium, u^μ is a timelike unit vector that describes its collective motion.

We can define the Local Rest Frame (LRF) of the medium as the frame in which $u^\mu = (1, 0, 0, 0)$.

There are two established ways to determine the flow u^μ and hence the LRF. We shall first look at the choice of C. Eckart [10], defined in terms of the particle flow,

$$u^\mu = \frac{N^\mu}{(N^\nu N_\nu)^{\frac{1}{2}}}. \tag{21}$$

Noting that the spatial components $\boldsymbol{u}$ are parallel to those of the particle flux, we can see that in the local rest frame by Eckart's definition

$$N^i_{(Eckart)} = 0, i = 1, 2, 3. \tag{22}$$

An alternative approach due to Landau and Lifschitz relates the local rest frame to the momentum flux. In Eckart's LRF there is no particle flow; in the Landau-Lifschitz LRF there is no matter flow. Their hydrodynamic four-velocity is thus the timelike eigenvector of the energy-momentum tensor [9].

$$T^{\mu\nu}u_\nu = \epsilon u^\mu, \tag{23}$$

where ϵ is the local energy density; this can be rewritten as

$$u^\mu = \frac{T^{\mu\nu}u_\nu}{T_{\alpha\beta}u^\alpha u^\beta}. \tag{24}$$

2.4.1 Entropy

The entropy current is a measure of the degree of equilibriation of the system, and is given by

$$S^\mu(x) = -\int \frac{d^3p}{p^0} p^\mu \Phi[f(x,\boldsymbol{p})], \tag{25}$$

where

$$\Phi[f(x,p)] \equiv f\ln f - \frac{1}{\varepsilon}(1+\varepsilon f)\ln(1+\varepsilon f). \tag{26}$$

and $\varepsilon = 1$ for bosons and -1 for fermions. For the classical limit, one may set $\varepsilon \to 0$ and

$$\Phi[f(x,p)] = f(\ln f - 1). \tag{27}$$

The covariant form of the second law of thermodynamics reads

$$\partial_\mu S^\mu \geq 0. \tag{28}$$

In section 2.7 we will discuss Boltzmann's H-theorem, which shows that this condition drives the evolution of closed systems toward a unique equilibrium.

2.5 Derivation of the Boltzmann Transport Equation

The Boltzmann equation was originally formulated to describe the evolution of a gas of classical particles, with the quantum generalization following later. We follow history in first deriving the classical equation along the lines of [11]; we will then extend it to QCD.

Recall from the definition of the distribution function $f(\boldsymbol{x}, \boldsymbol{p}, t)$ that the number of particles found at time t in the phase space element $d\mu \equiv d^3x d^3p/(2\pi)^3$ is given by $f(\boldsymbol{x}, \boldsymbol{p}, t)d\mu$. In particular, the total number of particles is given by

$$N = \int f(\boldsymbol{x}, \boldsymbol{p}, t) d\mu. \tag{29}$$

We follow the "motion" of a volume element in phase space from t to $t + dt$. We denote the volume element which develops after the time interval dt by $d\mu' \equiv d^3x' d^3p'/(2\pi)^3$. Then by Liouville's Theorem [12] we have

$$d\mu = d\mu'. \tag{30}$$

Now, the number of particles in $d\mu$ at time t is $f(\boldsymbol{x}, \boldsymbol{p}, t)d\mu$, and the number

of particles in $d\mu'$ at $t + dt$ is $f(\boldsymbol{x} + \boldsymbol{v}dt, \boldsymbol{p} + \boldsymbol{F}dt, t + dt)d\mu'$. Here $\boldsymbol{F}$ is an external force. At equilibrium (or in the absence of particle interactions), these particle numbers are identical. In general however, they may change due to scattering in/out of the phase space cell,

$$\left[f(\boldsymbol{x} + \boldsymbol{v}dt, \boldsymbol{p} + \boldsymbol{F}dt, t + dt) - f(\boldsymbol{x}, \boldsymbol{p}, t)\right] d\mu = N_{gain} - N_{loss} \equiv C[f]d\mu. \quad (31)$$

Here we have used Liouville's theorem to group the terms on the left. The right hand side is called the collision term, which is a functional of f, and accounts for particles entering or leaving the phase space element due to interactions.

We can recognize that the term in brackets on the left hand side (called the 'flow term') is simply the convective derivative

$$D_t f = \left[\partial_t + \boldsymbol{v} \cdot \boldsymbol{\nabla}_x + \boldsymbol{F}(\boldsymbol{x}) \cdot \boldsymbol{\nabla}_p\right] f(\boldsymbol{x}, \boldsymbol{p}, t). \quad (32)$$

The following expression for $C[f]$ is Boltzmann's famous *Stosszahlansatz*.

$$\begin{aligned} C[f] = \int d^3p_2 d^3p_3 d^3p_4 W(\boldsymbol{p}_1, \boldsymbol{p}_2; \boldsymbol{p}_3, \boldsymbol{p}_4) \Big[& f(\boldsymbol{x}, \boldsymbol{p}_3, t) f(\boldsymbol{x}, \boldsymbol{p}_4, t) \\ & - f(\boldsymbol{x}, \boldsymbol{p}_1, t) f(\boldsymbol{x}, \boldsymbol{p}_2, t) \Big], \end{aligned} \quad (33)$$

where the $\boldsymbol{p_i}$ label the incoming and outgoing momenta as in the following diagram of a general $2 \to 2$ collision.

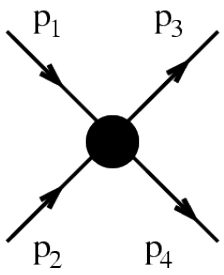

Figure 2: A general $2 \to 2$ scattering process

The *transition probability* $W(\boldsymbol{p}_1, \boldsymbol{p}_2; \boldsymbol{p}_3, \boldsymbol{p}_4)$ is the probability that in a collision two particles with initial momenta $\boldsymbol{p}_1$ and $\boldsymbol{p}_2$ will have final momenta $\boldsymbol{p}_3$ and $\boldsymbol{p}_4$.

We can identify the terms in the integrand of (33) with the gain and loss terms of Eq. (31).

Altogether we have the nonlinear integro-differential Boltzmann equation,

$$\begin{aligned} D_t f = \int d^3p_2 d^3p_3 d^3p_4 W(\boldsymbol{p}_1, \boldsymbol{p}_2; \boldsymbol{p}_3, \boldsymbol{p}_4) \Big[& f(\boldsymbol{x}, \boldsymbol{p}_3, t) f(\boldsymbol{x}, \boldsymbol{p}_4, t) \\ & - f(\boldsymbol{x}, \boldsymbol{p}_1, t) f(\boldsymbol{x}, \boldsymbol{p}_2, t) \Big]. \end{aligned} \tag{34}$$

By the H-theorem, a system that evolves according to this equation will equilibriate to the Boltzmann distribution.

$$f_B(p) = e^{\frac{p^2}{2mkT}}. \tag{35}$$

Indeed, evaluating the collision term (33) for f_B gives zero. It is quick to

show that this is a consequence of energy conservation in $2 \to 2$ collisions.

2.6 Generalization

We can generalize the classical equation (34) using the appropriate QCD matrix element for the transition probability and taking into account the effects of Bose statistics in the gain and loss terms, following Uehling and Uhlenbeck [13],

$$C[f] = \frac{1}{2}\int \frac{d^3p_2}{(2\pi)^2 2E_2}\frac{d^3p_3}{(2\pi)^2 2E_3}\frac{d^3p_4}{(2\pi)^2 2E_4}\frac{1}{2E_1}|\mathcal{M}_{12\to 34}|^2 \times \\ \times (2\pi)^4\delta(p_1+p_2-p_3-p_4)(f_3 f_4 \bar{f}_1 \bar{f}_2 - f_1 f_2 \bar{f}_3 \bar{f}_4). \tag{36}$$

Here the symmetry factor of $\frac{1}{2}$ corrects the double counting of final states in averaging spin, color and momentum. We use f_i as shorthand for $f(p_i)$ and in turn $\bar{f}_i$ as shorthand for $1 + f_i$. The $1 + f_i$ terms represent Bose-enhancement; more generally we could write $\bar{f} \equiv 1 + \varepsilon f$ where ε can be set to -1 to have the equation describe fermions. In this case the term accounts for Pauli blocking.

The transition probability (W in Eq. (34)) is expanded in terms of the matrix element for gluon-gluon scattering ($1 + 2 \to 3 + 4$) summed over spin and colour of particles 2,3 and 4 and averaged over spin and colour of particle 1 [14],

$$|\mathcal{M}_{12\to 34}|^2 = 72g^4\left[3 - \frac{tu}{s^2} - \frac{su}{t^2} - \frac{st}{u^2}\right], \tag{37}$$

where the dimensionless constant g is related to the QCD coupling constant α by

$$\alpha = \frac{g^2}{4\pi}, \tag{38}$$

and s, t and u are the usual Mandelstam variables (see Figure 2 for the labeling),

$$\begin{aligned} t &= (p_1 - p_3)^2 = (p_2 - p_4)^2 \\ s &= (p_1 + p_2)^2 = (p_4 + p_3)^2 \\ u &= (p_2 - p_3)^2 = (p_4 - p_1)^2. \end{aligned} \tag{39}$$

The delta function in (36) of course expresses energy-momentum conservation.

2.7 The equilibrium distribution function

The Boltzmann equation describes the evolution of an initial distribution function toward equilibrium. In this section we identify the form of equilibrium distribution function which would remain unchanged under this evolution. In the next section we will go a step further and show that in fact any initial condition is inevitably driven to this unique equilibrium distribution.

At equilibrium, the collision term of the Boltzmann equation is identically zero. In other words, the "gain" and "loss" terms from the integrand in Eq. (36) are equal; some refer to this as the "detailed balance condition",

$$f_3 f_4 \bar{f}_1 \bar{f}_2 = \bar{f}_3 \bar{f}_4 f_1 f_2. \tag{40}$$

Taking the logarithm of both sides and rearranging we have

$$\ln \frac{f_3}{\bar{f}_3} + \ln \frac{f_4}{\bar{f}_4} = \ln \frac{f_1}{\bar{f}_1} + \ln \frac{f_2}{\bar{f}_2}. \tag{41}$$

With ingoing particles on one side and outgoing particles on the other, this equation seems to imply that the expression $\ln\left(f_i/\bar{f}_i\right)$ is related to the invariants of the collision. Now for systems with only one type of particle in which particle number, energy and momentum are conserved, the general form of the collision invariants Ψ_i is [15]

$$\Psi_i = a(x) + b_\mu(x) p_i^\mu \tag{42}$$

It is easy to verify that the expression

$$f_{eq}(x,p) = \left[e^{-a(x)-b_\mu p^\mu} - \varepsilon\right]^{-1} \tag{43}$$

satisfies the required condition (41).

Identifying $a(x) = \frac{\mu(x)}{T(x)}$ and $b_\mu(x) = -\frac{u_\mu(x)}{T(x)}$ we obtain the Jüttner equilibrium distribution [16]

$$f_{eq}(x,p) = \left[e^{\frac{p^\mu u_\mu(x) - \mu(x)}{T(x)}} - \varepsilon\right]^{-1}. \tag{44}$$

Here T, u and μ parameterize the temperature, collective flow velocity and chemical potential, respectively.

From this distribution we can calculate the total particle number, momentum and energy densities at equilibrium, choosing our coordinate system such that $\boldsymbol{u} \equiv (0, 0, u)$ coincides with the z-axis. Then,

$$n_{eq} = \frac{\gamma T^3}{\pi^2} \operatorname{Li}_3(e^{\frac{\mu}{T}}), \tag{45}$$

$$p_{eq} = -\frac{4\gamma^2 T^4}{\pi^2} \operatorname{Li}_4(e^{\frac{\mu}{T}}), \tag{46}$$

$$\epsilon_{eq} = \frac{\gamma^2 T^4 (u^2 + 3)}{\pi^2} \operatorname{Li}_4(e^{\frac{\mu}{T}}). \tag{47}$$

Here $\operatorname{Li}_s(z)$ is the polylogarithm of order s, which we define in the appendices (see section 7.1).

Calculating these parameters for a given initial distribution function, we can equate them to the above expressions and solve simultaneously in order to find the corresponding (unique) equilibrium parameters T, μ and u.

2.8 The H-Theorem and thermal equilibrium

In this section we will show for the special case of a spatially homogeneous systen of bosons that given the covariant second law of thermodynamics (28), an arbitrary distribution function evolved in time according to the Boltzmann equation will be driven to the equilibrium Jüttner distribution.

Following [17], we begin by establishing some inequalities that we will need later. First, for positive real y,

$$(y-1) - \ln y \geq 0. \tag{48}$$

Proof: Differentiating the LHS we obtain $1 - 1/y$. Setting this to zero we find that the function has one extremum at $y = 1$, for which value the LHS $= 0$. From the positive sign of the second derivative $1/y^2$ we conclude that this is a local minimum.

Setting $y = 1/x$ and multiplying (48) by x, we find

$$x \ln x + 1 - x \geq 0. \tag{49}$$

We further make the claim [17] that for all $x > 0$ there exists a constant C such that

$$x \ln x + 1 - x - CG(|x-1|)|x-1| \geq 0, \tag{50}$$

where

$$G(|x-1|) = \begin{cases} |x-1|, & \text{if } 0 \leq |x-1| \leq 1, \\ 1, & \text{if } |x-1| \geq 1. \end{cases} \tag{51}$$

Boltzmann's quantity H^μ, originally named for "heat", is related (by definition) to the entropy (25) very simply in natural units by

$$H^\mu = -S^\mu. \tag{52}$$

Recalling the balance equation (28) for S^μ, we have that

$$\partial_\mu H^\mu \leq 0. \tag{53}$$

We now introduce the scalar invariant

$$H \equiv u_\mu H^\mu, \tag{54}$$

where u^μ is the collective flow velocity. Evaluating this in the rest frame we see that

$$H = H^0 = \int \frac{d^3p}{p_0} p_0 f \ln f - \bar{f} \ln \bar{f}. \tag{55}$$

From our assumption of spatial homogeneity, we find that (53) reduces to

$$\frac{dH}{dt} \leq 0. \tag{56}$$

Thus we can infer that H decreases over time. Further, the time derivative of H vanishes when at equilibrium. We denote the equilibrium value of H by $H_{eq} \equiv H[f_{eq}]$.

Now, consider the auxiliary relations (48) and (49), choosing

$$y = \frac{\bar{f}}{\bar{f}_{eq}}; \quad x = \frac{f}{\bar{f}}\frac{\bar{f}_{eq}}{f_{eq}}. \tag{57}$$

Adding the two resulting inequalities, we get

$$f\left[\ln\left(\frac{f}{\bar{f}}\right) - \ln\left(\frac{f_{eq}}{\bar{f}_{eq}}\right)\right] - \ln\left(\frac{\bar{f}}{\bar{f}_{eq}}\right) \geq 0. \tag{58}$$

Multiplying by p^0 and integrating over all values of d^3p/p^0 we obtain

$$H - H_{eq} \geq \int p^0 \frac{d^3p}{p^0}(f - f_{eq}) \ln\left(\frac{f_{eq}}{\bar{f}_{eq}}\right). \tag{59}$$

Substituting the equilibrium distribution

$$f_{eq} = \frac{1}{e^{\frac{1}{T}(u^\alpha p_\alpha - \mu)} - 1}, \tag{60}$$

we can write

$$\ln\left(\frac{f_{eq}}{\bar{f}_{eq}}\right) = -\frac{1}{T}(u^\alpha p_\alpha - \mu). \tag{61}$$

Altogether,

$$H - H_{eq} \geq -u^\alpha \int \frac{d^3p}{p^0} p_\alpha (f - f_{eq}) \frac{1}{T}(u^\beta p_\beta - \mu). \tag{62}$$

Imposing the conditions

$$u_\mu J^\mu = u_\mu J^\mu_{eq}, \quad u_\mu u_\nu T^{\mu\nu} = u_\mu u_\nu T^{\mu\nu}_{eq}, \tag{63}$$

the right side of the inequality (62) vanishes. Thus we have that

$$H \geq H_{eq}. \tag{64}$$

In other words, H is bounded from below by H_{eq}. Since $\frac{dH}{dt}$ is in general negative and vanishes when the distribution function is the equilibrium one, we expect that $H \to H_{eq}$ as $t \to \infty$. For a rigorous proof of this expectation, see [17]. We will assume it is true in order to prove that f evolves to f_{eq} for systems governed by the Boltzmann equation.

This time making use of (50) we write

$$f\left[\ln\left(\frac{f}{\bar{f}}\right) - \ln\left(\frac{f_{eq}}{\bar{f}_{eq}}\right)\right] - \ln\left(\frac{\bar{f}}{\bar{f}_{eq}}\right) - CG\left(\frac{|f_{eq}-f|}{f_{eq}(\bar{f})}\right)\frac{|f_{eq}-f|}{\bar{f}_{eq}} \geq 0. \tag{65}$$

Following a similar procedure to the previous inequality, we integrate over d^3p and derive

$$H - H_{eq} \geq C\left[\int_{L_t} \frac{d^3p}{p^0} p^0 \frac{|f_{eq}-f|}{\bar{f}_{eq}} + \int_{S_t} \frac{d^3p}{p^0} p^0 \frac{|f_{eq}-f|^2}{f_{eq}\bar{f}\bar{f}_{eq}}\right]. \tag{66}$$

Here L_t and S_t denote the integration domains where $|f_{eq} - f| > f_{eq}$ and $|f_{eq} - f| < f_{eq}$ respectively. As H tends to H_{eq} (which it must, by assumption) the sum of the integrals goes to 0. Since both integrands are positive, they must vanish independently in this limit.

Now by Schwarz's inequality, it can be shown that

$$\int_{S_t} \frac{d^3p}{p^0} p^0 \frac{|f_{eq} - f|}{\bar{f}_{eq}} \leq \left[\int_{S_t} \frac{d^3p}{p^0} p^0 \frac{f_{eq}(\bar{f})}{\bar{f}_{eq}}\right]^{\frac{1}{2}} \left[\int_{S_t} \frac{d^3p}{p^0} p^0 \frac{|f_{eq} - f|^2}{f_{eq}(\bar{f})(\bar{f}_{eq})}\right]^{\frac{1}{2}} \to 0 \tag{67}$$

when $t \to \infty$. Therefore the following integral (over the entire domain of integration) tends to 0 as $t \to \infty$,

$$\int \frac{d^3p}{p^0} p^0 \frac{|f_{eq} - f|}{\bar{f}_{eq}} = \int_{L_t} \frac{d^3p}{p^0} p^0 \frac{|f_{eq} - f|}{\bar{f}_{eq}} + \int_{S_t} \frac{d^3p}{p^0} p^0 \frac{|f_{eq} - f|}{\bar{f}_{eq}} \to 0 \tag{68}$$

from which we can conclude, as anticipated, that f tends strongly to f_{eq} in L^1 assuming that H tends to H_{eq} when $t \to \infty$.

2.9 Bose-Einstein condensation

It can be shown [1] that the systems of gluons created in the early stages of a relativistic heavy ion collision may contain more gluons than can be accomodated in a Bose-Einstein equilibrium distribution. Furthermore it has been argued that under the assumption of approximate gluon number conservation, a transient equilibrium state may form with a Bose-Einstein condensate in order to accommodate them. We will illustrate this with an example, assuming number conservation.

Now, it should be noted that for a given initial condition, the parameters that define the equilibrium distribution are fully determined by conservation

laws. To demonstrate this, consider a family of spherically symmetric initial conditions

$$f(p) = f_0\theta(1 - p/Q_s), \tag{69}$$

where f_0 is a density parameter, θ is the Heaviside step function and Q_s sets a typical momentum scale. Now, the initial particle number and energy densities are

$$n_0 = f_0\frac{1}{2\pi^2}\int_0^{Q_s} dp\, p^2 = f_0\frac{Q_s^3}{6\pi^2}, \tag{70}$$

and

$$\epsilon_0 = f_0\frac{1}{2\pi^2}\int_0^{Q_s} dp\, p^3 = f_0\frac{Q_s^4}{8\pi^2}. \tag{71}$$

Now consider the number and energy densities for the equilibrium Bose distribution. From Eq. (45) and (47) we have

$$n_{eq}(T,\mu) = \frac{T^3}{\pi^2}\,\mathrm{Li}_3(e^{\mu/T}), \tag{72}$$

and

$$\epsilon_{eq}(T,\mu) = \frac{3T^4}{\pi^2}\,\mathrm{Li}_4(e^{\mu/T}). \tag{73}$$

By particle number and energy conservation, $n_0 = n_{eq}$ and $\epsilon_0 = \epsilon_{eq}$, which we can solve for the equilibrium parameters μ and T.

Note that for massless bosons, the chemical potential μ must be strictly negative.[1] Now, it is observed that increasing f_0 in the initial condition correspondingly increases μ in the final equilibrium state until $\mu = 0$. Beyond this point, the "excess gluons" must populate the condensate - see Fig 3.

We can find this critical value of f_0 by setting $\mu = 0$ in (70) and (71), in which case

$$n_{eq}(T, 0) = \frac{\zeta(3)}{\pi^2} T^3, \tag{74}$$

and

$$\epsilon_{eq}(T, 0) = 3\zeta(4)T^4 = \frac{\pi^2}{30} T^4, \tag{75}$$

where $\zeta(x) \equiv \sum_{n=1}^{\infty} \frac{1}{n^x}$ is the Riemann Zeta function.

We can write down a dimensionless combination of the particle number and energy densities $n_{eq}\epsilon_{eq}^{-3/4} = \frac{30^{3/4}\zeta(3)}{\pi^{7/2}} \approx 0.28$.

A condensate will develop when $n_0\epsilon_0^{-3/4} \geq n_{eq}\epsilon_{eq}^{-3/4}$ [1]. Evaluating this numerically, the critical value for our family of initial conditions (69) at

[1] Usually of course at equilibrium we would expect μ to be zero, but this is a consequence of variable gluon number. The "equilibrium" reached under our assumption of gluon number conservation is a transient state, with full chemical equilibrium ($\mu = 0$) being reached subsequently.

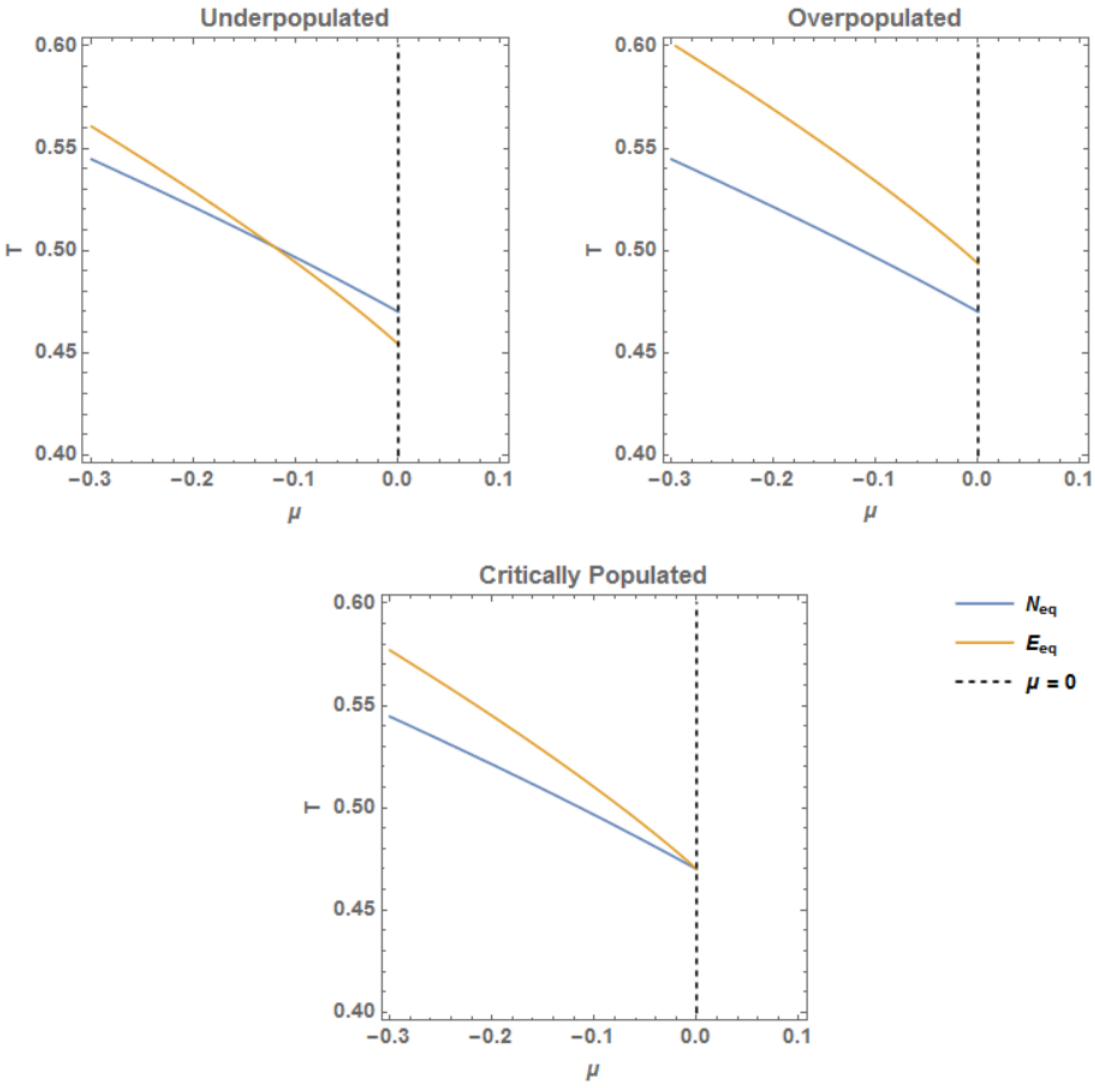

Figure 3: Contours of constant particle number (70) and energy density (71) at equilibrium. In the under- and critically populated cases, the values of the equilibrium parameters T and μ are found where the lines intersect. In the critically populated case, the intersection occurs at the maximum possible value of $\mu = 0$. In the overpopulated case, no solution for $\mu < 0$ exists and a condensate is necessary to contain the excess particles.

which condensation occurs is $f_0^c \approx 0.157$

2.9.1 A kinematic subtlety

It is worth pointing out a subtlety regarding the conclusion from Sec. 2.9 that a condensate may form in finite time. The Mandelstam variables (39) read for vanishing mass

$$\begin{aligned} s &= (p_1 + p_2)^2 = (p_3 + p_4)^2 = 2p_1.p_2 = 2p_3.p_4 \\ t &= (p_1 - p_3)^2 = (p_2 - p_4)^2 = 2p_1.p_3 = 2p_2.p_4 \\ u &= (p_2 - p_3)^2 = (p_4 - p_1)^2 = 2p_2.p_3 = 2p_4.p_1 \end{aligned} \tag{76}$$

In order for the Bose-Einstein condensate to form, we must have that one of the outgoing particles is scattered into a zero-momentum state. Without loss of generality, suppose $\boldsymbol{p}_4 = 0$, i.e. the 4-vector p_4 vanishes.

Then all Mandelstam variables (s, t and u) vanish identically. In particular, $t = 0$ holds only for nonzero momenta $\boldsymbol{p}_1, \boldsymbol{p}_2$ if the momenta are parallel, as

$$\begin{aligned} t &= 2p_1.p_3 \\ &= 2(E_1 E_3 - \boldsymbol{p}_1 \cdot \boldsymbol{p}_3) = 0. \end{aligned} \tag{77}$$

However, this condition corresponds to a hypersurface in the accessible phase space of measure zero. This implies that scatterings into the condensate will not occur for finite matrix elements M^2, like the often used model

$$M^2 \propto s^2/(t - \mu^2)^2, \tag{78}$$

which describes, for the dominant t-channel contribution, relevant screening effects not included in the tree-level approximation (37).

However, as analyzed in [18], a matrix element with

$$M^2 \propto s^2/t(t-\mu^2), \tag{79}$$

which diverges as $t \to 0$, however less strongly than the tree-level approximation (37) where $M^2 \propto 1/t^2$, yields a non-zero probability for scatterings into the condensate. The ansatz (79) is inspired by HTL sum rules, and it gives the same behaviour for purposes of the approximation to be derived in Sec. 3.

Another (not unrelated) possibility of a non-zero scattering rate into the condensate emerges [1][19] when taking into account the fact that gluons in the medium acquire a dynamical mass, which directly lifts the kinematic constraint (77).

3 The Fokker-Planck Equation

3.1 The Small-Scattering Angle Approximation

Under the assumption that small scattering angles dominate, it is possible to simplify the Boltzmann equation, writing it as a Fokker-Planck equation. Originally developed by Adriaan Fokker [20] and Max Planck [21] to describe the time evolution of the velocity of a classical particle undergoing Brownian motion, for our purposes we will interpret it as describing the distribution function of the gluon plasma.

Starting from the collision term (36), we rewrite the momenta p_i in terms of the momentum transfer q, viz.

$$p_3 = p_1 + q; \quad p_4 = p_2 - q. \tag{80}$$

We use our substitution and the 3-momentum components of the delta function to rewrite the integrals over p_3 and p_4 in terms of q. The collision term then becomes

$$C[f] = \int_{p_2} \int_q W(p_1, p_2, q)(f_3 f_4 \bar{f}_1 \bar{f}_2 - f_1 f_2 \bar{f}_3 \bar{f}_4), \tag{81}$$

where

$$W(p_1, p_2, q) \equiv \frac{1}{128\pi^2} \frac{\delta(E_1 + E_2 - E_3 - E_4)}{E_1 E_2 E_3 E_4} |\mathcal{M}_{12\to 34}|^2. \tag{82}$$

Now assuming that the momentum transfer q is small, we can make the expansion

$$f_3 \equiv f(\boldsymbol{p}_3) = f(\boldsymbol{p}_1 + \boldsymbol{q}) \approx f_1 + \boldsymbol{q} \cdot \boldsymbol{\nabla} f_1 \tag{83}$$

and similarly

$$f_4 \approx f_2 - \boldsymbol{q} \cdot \boldsymbol{\nabla} f_2. \tag{84}$$

Then

$$\begin{aligned} \bar{f}_1 \bar{f}_2 f_3 f_4 - f_1 f_2 \bar{f}_3 \bar{f}_4 \approx & \bar{f}_1 \bar{f}_2 (f_1 + \boldsymbol{q} \cdot \boldsymbol{\nabla} f_1)(f_2 - \boldsymbol{q} \cdot \boldsymbol{\nabla} f_2) \\ & - f_1 f_2 (\bar{f}_1 + \boldsymbol{q} \cdot \boldsymbol{\nabla} f_1)(\bar{f}_2 - \boldsymbol{q} \cdot \boldsymbol{\nabla} f_2) \\ & = f_1 f_2 \bar{f}_1 \bar{f}_2 - \bar{f}_1 \bar{f}_2 f_1 \boldsymbol{q} \cdot \boldsymbol{\nabla} f_2 + \bar{f}_1 \bar{f}_2 f_2 \boldsymbol{q} \cdot \boldsymbol{\nabla} f_1 \\ & - f_1 f_2 \bar{f}_1 \bar{f}_2 + f_1 f_2 \bar{f}_1 \boldsymbol{q} \cdot \boldsymbol{\nabla} f_2 - f_1 f_2 \bar{f}_2 \boldsymbol{q} \cdot \boldsymbol{\nabla} f_1 \\ & . \end{aligned} \tag{85}$$

Defining $h_i \equiv f_i \bar{f}_i$, we can write the above as

$$\begin{aligned} & - h_1 \bar{f}_2 \boldsymbol{q} \cdot \boldsymbol{\nabla} f_2 + \bar{f}_1 h_2 \boldsymbol{q} \cdot \boldsymbol{\nabla} f_1 - h_1 f_2 \boldsymbol{q} \cdot \boldsymbol{\nabla} f_2 - f_1 h_2 \boldsymbol{q} \cdot \boldsymbol{\nabla} f_1 \\ =& h_1 (f_2 - \bar{f}_2) \boldsymbol{q} \cdot \boldsymbol{\nabla} f_2 + h_2 (\bar{f}_1 - f_1) \boldsymbol{q} \cdot \boldsymbol{\nabla} f_1 \\ =& q \cdot (h_2 \boldsymbol{\nabla} f_1 - h_1 \boldsymbol{\nabla} f_2). \end{aligned} \tag{86}$$

For small scattering angles, the matrix element is dominated by small values of t and/or u and can be simplified. Performing the integral over q, it is

possible to write the result as the divergence of a current in momentum space [1],

$$D_t f = -\boldsymbol{\nabla} \cdot \mathcal{J}(\boldsymbol{p}), \tag{87}$$

where $\mathcal{J}$ can be found to be

$$\mathcal{J}_i(\boldsymbol{p}) = \frac{9}{4\pi} g^4 \mathcal{L} \int_{\boldsymbol{k}} \mathcal{V}_{ij}(\boldsymbol{p}, \boldsymbol{k}) \left\{ f_p \bar{f}_p \nabla_k^j f_k - f_k \bar{f}_k \nabla_p^j f_p \right\}. \tag{88}$$

Introduced here is

$$\mathcal{V}^{ij} = (1 - \boldsymbol{v} \cdot \boldsymbol{w})\, \delta^{ij} + \left(v^i w^j + v^j w^i \right), \tag{89}$$

where to lighten notation we have defined $\boldsymbol{p} \equiv \boldsymbol{p}_1$, $\boldsymbol{k} \equiv \boldsymbol{p}_2$ and denoted the corresponding unit vectors by $\boldsymbol{w} \equiv \boldsymbol{p}/p$ and $\boldsymbol{v} \equiv \boldsymbol{k}/k$.

In Eq. (88), $\mathcal{L}$ is the characteristic Coulomb logarithm emerging in screened interactions with vector boson exchange, $\mathcal{L} = \int_{q_{min}}^{q_{max}} \frac{dq}{q} = \ln \frac{q_{max}}{q_{min}}$ where q_{max} and q_{min} are cutoffs of the order of the equilibrium temperature T and Debye screening mass m_D, respectively [1]. We take $\mathcal{L}$ to be a constant parameter in our analysis.

3.2 Spherical symmetry

For an isotropic momentum distribution, the integral (88) can be performed (see the next section for a more general step-by-step calculation of the integral

valid also for cylindrically symmetric distributions) and yields [1]

$$\mathcal{J}(\boldsymbol{p}) = -2\pi^2\alpha^2\xi\left[I_a\nabla f(\boldsymbol{p}) + \frac{\boldsymbol{p}}{p}I_b f(\boldsymbol{p})[1+f(\boldsymbol{p})]\right], \tag{90}$$

where $\xi \equiv \frac{18\mathcal{L}}{\pi}$. Note that $\mathcal{L}$ via ξ in (90) determines the time scale of the evolution.

I_a and I_b are functionals of the distribution function,

$$I_a \equiv \int \frac{d^3p}{(2\pi)^3} f(\boldsymbol{p})(1+f(\boldsymbol{p})), \tag{91}$$

and

$$I_b \equiv \int \frac{d^3p}{(2\pi)^3}\frac{2f(\boldsymbol{p})}{p}. \tag{92}$$

I_a plays the role of a diffusion constant (it is the proportionality coefficient between the current and the gradient of f to within numerical constants), while I_b is proportional to the square of the off-equilibrium Debye screening mass,

$$m_D^2 = 2g^2 N_c I_b. \tag{93}$$

It is convenient to rescale the time variable as

$$\tau \equiv 2\pi^2\alpha^2\xi t. \tag{94}$$

The Fokker-Planck equation then reads

$$D_\tau f(\tau, \boldsymbol{p}) = \boldsymbol{\nabla} \cdot \left[I_a \boldsymbol{\nabla} f(\tau, \boldsymbol{p}) + \frac{\boldsymbol{p}}{p} I_b f(\tau, \boldsymbol{p})[1 + f(\tau, \boldsymbol{p})] \right]. \tag{95}$$

As we are assuming an isotropic system without spatial dependence or external forces, the derivative and gradient terms can be simplified, and Eq. (95) reduces to

$$\partial_\tau f(\tau, p) = I_a \frac{\partial^2 f}{\partial p^2} + \frac{2I_b}{p} f(1 + f) + \left[\frac{2I_a}{p} + I_b(1 + 2f) \right] \frac{\partial f}{\partial p}. \tag{96}$$

Note that I_a and I_b depend on the distribution function over all momenta, not just the value we evaluate the current for. The transport equation is thus non-local in momentum space and also non-linear as I_a and I_b are quadratic and linear functionals of f respectively.

We can write (96) in terms of the current as

$$\partial_\tau f(\tau, p) = -\frac{1}{p^2} \frac{\partial}{\partial p} (p^2 \mathcal{J}(\tau, p)), \tag{97}$$

where $\mathcal{J}(\tau, p)$ is given by

$$\mathcal{J}(\tau, p) = -I_a \partial_p f - I_b f(1 + f). \tag{98}$$

Now, by the H-theorem we expect that the system of gluons will evolve from any initial condition to the equilibrium Bose distribution

$$f_{eq}(p) = \frac{1}{e^{(p-\mu)/T} - 1}, \tag{99}$$

where μ and T are the equilibrium parameters that can be simply calculated from the initial condition by invoking energy/particle number conservation, as detailed in Sec. 2.7.

An important relation between I_a and I_b at equilibrium can be found by noting that $\frac{\partial f_{eq}}{\partial p} = -f_{eq}(1 + f_{eq})/T$ and hence (integrating Eq. (92) by parts and comparing to (91))

$$I_b[f_{eq}] = -\int \frac{d^3p}{(2\pi)^3} 2f \left(\frac{\partial f_{eq}}{\partial p}\right) = \frac{1}{T} I_a[f_{eq}]. \tag{100}$$

This relation shows explicitly that the current vanishes identically at equilibrium, and that f_{eq} is therefore indeed the stationary solution of the Boltzmann equation, as one might expect from the H-theorem.

3.3 Cylindrical symmetry

The previous section was a review of the work of Blaizot et al. [1]. We wish to extend it, beginning by determining the current for a more general, cylindrically symmetric momentum distribution. (The following calculations are our own.)

Starting from Eq. (88), we can rewrite the current, grouping the constants and taking the factors that do not depend on $\boldsymbol{k}$ out of the integral,

$$\mathcal{J}_i(\boldsymbol{p}) = C f_p \bar{f}_p \int_{\boldsymbol{k}} \mathcal{V}_{ij} \nabla_k^j f_k - C \nabla_p^j f_p \int_{\boldsymbol{k}} \mathcal{V}_{ij} f_k \bar{f}_k, \tag{101}$$

where we have defined $C \equiv \frac{9}{4\pi} g^4 \mathcal{L}$.

The two integrals correspond to a vector quantity

$$J_i \equiv \int_{\boldsymbol{k}} \mathcal{V}_{ij} \nabla_k^j f_k, \tag{102}$$

and a tensor quantity

$$\mathbb{J}_{ij} = \int_{\boldsymbol{k}} \mathcal{V}_{ij} f_k \bar{f}_k. \tag{103}$$

The current $\mathcal{J}$ depends on momentum $\boldsymbol{p}$ whose orientation relative to the direction of the flow $\boldsymbol{u}$ is fixed. For this $\boldsymbol{p}$ we then integrate over all possible values of $\boldsymbol{k}$. To that end we choose our coordinates such that the z-axis lies along $\boldsymbol{u}$ and $\phi_p = 0$, i.e. $\boldsymbol{p}$ lies in the xz-plane. Thus in Cartesian coordinates,

$$\boldsymbol{p} = (p_\perp, 0, p_z), \tag{104}$$

and

$$\boldsymbol{k} = (k_\perp \cos\phi_k, k_\perp \sin\phi_k, k_z). \tag{105}$$

Since we describe massless gluons, the magnitude of the corresponding velocities is unity, thus

$$\boldsymbol{w} = \frac{\boldsymbol{p}}{p} = \frac{1}{\sqrt{p_\perp^2 + p_z^2}} \left(p_\perp, 0, p_z\right), \tag{106}$$

and similarly

$$\boldsymbol{v} = \frac{1}{\sqrt{k_\perp^2 + k_z^2}} \left(k_\perp \cos\phi_k, k_\perp \sin\phi_k, k_z\right). \tag{107}$$

For the sake of notational convenience, define $w \equiv \frac{p_z}{\sqrt{p_\perp^2+p_z^2}}$, $\tilde{w} = \sqrt{1-w^2}$, $v \equiv \frac{k_z}{\sqrt{k_\perp^2+k_z^2}}$ and $\tilde{v} = \sqrt{1-v^2}$. Then $\boldsymbol{v} = (\tilde{v}\cos\phi_k, \tilde{v}\sin\phi_k, v)$ and $\boldsymbol{w} = (\tilde{w}, 0, w)$.

Using these definitions, we can represent the $\mathcal{V}_{ij}$ tensor as a matrix,

$$\mathcal{V}_{ij} = \begin{pmatrix} 1 - vw + \tilde{v}\tilde{w}\cos\phi_k & \tilde{v}\tilde{w}\sin\phi_k & v\tilde{w} + \tilde{v}w\cos\phi_k \\ \tilde{v}\tilde{w}\sin\phi_k & 1 - vw - \tilde{v}\tilde{w}\cos\phi_k & \tilde{v}w\sin\phi_k \\ v\tilde{w} + \tilde{v}w\cos\phi_k & \tilde{v}w\sin\phi_k & 1 + vw - \tilde{v}\tilde{w}\cos\phi_k \end{pmatrix}. \tag{108}$$

Since the current $\mathcal{J}(\boldsymbol{p})$ lies in the xz-plane, $J_\perp = J_x$ by construction.

Expanding the gradient in Eq. (102) in terms of Cartesian unit vectors and cylindrical partial derivatives, we have

$$\boldsymbol{\nabla}_k f_k = \frac{\partial f_k}{\partial k_\perp}\cos\phi_k \hat{x} + \frac{\partial f_k}{\partial k_\perp}\sin\phi_k \hat{y} + \frac{\partial f_k}{\partial k_z}\hat{z}. \tag{109}$$

Thus for the relevant components 1 and 3,

$$\mathcal{V}_{1j}\nabla_k^j f_k = \begin{pmatrix} 1 - vw + \tilde{v}\tilde{w}\cos\phi_k & \tilde{v}\tilde{w}\sin\phi_k & v\tilde{w} + \tilde{v}w\cos\phi_k \end{pmatrix} \begin{pmatrix} \frac{\partial f_k}{\partial k_\perp}\cos\phi_k \\ \frac{\partial f_k}{\partial k_\perp}\sin\phi_k \\ \frac{\partial f_k}{\partial k_z} \end{pmatrix}$$
$$= \tilde{v}\tilde{w}\frac{\partial f_k}{\partial k_\perp} + v\tilde{w}\frac{\partial f_k}{\partial k_z} + \cos\phi_k\left((1-vw)\frac{\partial f_k}{\partial k_\perp} + \tilde{v}w\frac{\partial f_k}{\partial k_z}\right), \tag{110}$$

and

$$\mathcal{V}_{3j}\nabla_k^j f_k = \begin{pmatrix} v\tilde{w} + \tilde{v}w\cos\phi_k & \tilde{v}w\sin\phi_k & 1 + vw - \tilde{v}\tilde{w}\cos\phi_k \end{pmatrix} \begin{pmatrix} \frac{\partial f_k}{\partial k_\perp}\cos\phi_k \\ \frac{\partial f_k}{\partial k_\perp}\sin\phi_k \\ \frac{\partial f_k}{\partial k_z} \end{pmatrix}$$
$$= \tilde{v}w\frac{\partial f_k}{\partial k_\perp} + (1+vw)\frac{\partial f_k}{\partial k_z} + \cos\phi_k\left(v\tilde{w}\frac{\partial f_k}{\partial k_\perp} - \tilde{v}\tilde{w}\frac{\partial f_k}{\partial k_z}\right). \tag{111}$$

Now $\int_0^{2\pi} d\phi\cos\phi = 0$, so the terms with a factor of $\cos\phi_k$ vanish under integration. This leaves no ϕ_k dependance in the J_i integrals in Eq. (102), so we simply pick up a factor of 2π from the integration over ϕ_k.

Altogether,

$$J_\perp = \frac{1}{(2\pi)^2}\int_{-\infty}^{\infty} dk_z \int_0^{\infty} dk_\perp k_\perp \left(\tilde{v}\tilde{w}\frac{\partial f_k}{\partial k_\perp} + v\tilde{w}\frac{\partial f_k}{\partial k_z}\right), \tag{112}$$

and

$$J_z = \frac{1}{(2\pi)^2}\int_{-\infty}^{\infty} dk_z \int_0^{\infty} dk_\perp k_\perp \left(\tilde{v}w\frac{\partial f_k}{\partial k_\perp} + (1+vw)\frac{\partial f_k}{\partial k_z}\right). \tag{113}$$

Now consider $\mathbb{J}_{ij} = \int_{\boldsymbol{k}} \mathcal{V}_{ij} f_k \bar{f}_k$. The components of the tensor are given by in Eq. (103) by integrals over the individual components of $\mathcal{V}_{ij}$ multiplied by $f_k \bar{f}_k$. As before, terms with a factor of $\cos\phi_k$ or $\sin\phi_k$ integrate to zero, so we can simplify the expression by removing them,

$$\mathbb{J}_{ij} = \frac{1}{(2\pi)^2} \int_{-\infty}^{\infty} dk_z \int_0^{\infty} dk_\perp k_\perp \begin{pmatrix} 1 - vw & 0 & v\tilde{w} \\ 0 & 1 - vw & 0 \\ v\tilde{w} & 0 & 1 + vw \end{pmatrix} f_k \bar{f}_k. \quad (114)$$

Henceforth we will use our general shorthand $\int$ in the form

$$\int \equiv \frac{1}{(2\pi)^2} \int_{-\infty}^{\infty} dk_z \int_0^{\infty} dk_\perp k_\perp, \quad (115)$$

specifically for the cylindrically symmetric case.

Expanding $\mathbb{J}_{ij} \nabla_p^j f_p$ for $i = 1, 3$ we have

$$\begin{aligned} \mathbb{J}_{1j} \nabla_p^j f_p &= \int \begin{pmatrix} 1 - vw, & 0, & v\tilde{w} \end{pmatrix} \begin{pmatrix} \frac{\partial f_p}{\partial p_\perp} \\ 0 \\ \frac{\partial f_p}{\partial p_z} \end{pmatrix} f_k \bar{f}_k \\ &= \frac{\partial f_p}{\partial p_\perp} \int (1 - vw) f_k \bar{f}_k + \frac{\partial f_p}{\partial p_z} \int v\tilde{w} f_k \bar{f}_k, \end{aligned} \quad (116)$$

and

$$\begin{aligned}\mathbb{J}_{3j}\nabla_p^j f_p &= \int \begin{pmatrix} v\tilde{w}, & 0, & 1+vw \end{pmatrix} \begin{pmatrix} \frac{\partial f_p}{\partial p_\perp} \\ 0 \\ \frac{\partial f_p}{\partial p_z} \end{pmatrix} f_k \bar{f}_k \\ &= \frac{\partial f_p}{\partial p_\perp} \int v\tilde{w} f_k \bar{f}_k + \frac{\partial f_p}{\partial p_z} \int (1+vw) f_k \bar{f}_k.\end{aligned} \tag{117}$$

Noting that we can take factors of w and $\tilde{w}$ (related to "external" momentum p) out of the integrals, the integrals that need to be performed are all of the form $\int f_k \bar{f}_k$, $\int v f_k \bar{f}_k$, $\int \frac{\partial f_k}{\partial k_z}$, $\int v \frac{\partial f_k}{\partial k_z}$ or $\int \tilde{v} \frac{\partial f_k}{\partial k_\perp}$.

Note that $\int_{-\infty}^{\infty} dk_z \frac{\partial f_k}{\partial k_z} = f_k|_{-\infty}^{\infty} = 0$ since we assume the distribution function vanishes for large momenta.

We can remove the remaining partial derivatives by integrating by parts,

$$\begin{aligned}\int_{-\infty}^{\infty} dk_z v \frac{\partial f_k}{\partial k_z} &= v f_k|_{-\infty}^{\infty} - \int_{-\infty}^{\infty} dk_z f_k \frac{\partial v}{\partial k_z} \\ &= -\int_{-\infty}^{\infty} dk_z f_k \frac{\partial}{\partial k_z} \left(\frac{k_z}{\sqrt{k_\perp^2 + k_z^2}} \right) \\ &= -\int_{-\infty}^{\infty} dk_z f_k \frac{k_\perp^2}{(k_\perp^2 + k_z^2)^{\frac{3}{2}}} \\ &= -\int_{-\infty}^{\infty} dk_z \tilde{v}^3 \frac{f_k}{k_\perp},\end{aligned} \tag{118}$$

and

$$\begin{aligned}
\int_0^\infty dk_\perp k_\perp \tilde{v}\frac{\partial f_k}{\partial k_\perp} &= k_\perp \tilde{v} f_k|_0^\infty - \int_0^\infty dk_\perp f_k \frac{\partial}{\partial k_\perp}(k_\perp \tilde{v}) \\
&= -\int_0^\infty dk_\perp f_k \frac{\partial}{\partial k_\perp}\left(\frac{k_\perp^2}{\sqrt{k_\perp^2+k_z^2}}\right) \\
&= -\int_0^\infty dk_\perp f_k \left(-\frac{k_\perp^3}{(k_\perp^2+k_z^2)^{\frac{3}{2}}} + \frac{2k_\perp}{\sqrt{k_\perp^2+k_z^2}}\right) \\
&= \int_0^\infty dk_\perp k_\perp (\tilde{v}^3 - 2\tilde{v})\frac{f_k}{k_\perp} \\
&= \int_0^\infty dk_\perp k_\perp \left(\tilde{v}^3 \frac{f_k}{k_\perp} - 2\frac{f_k}{k}\right).
\end{aligned} \tag{119}$$

Putting it all together, we can write down complete expressions for the current,

$$\begin{aligned}
\mathcal{J}_\perp(\boldsymbol{p})/C &= -\tilde{w} f_p \bar{f}_p \int \frac{2f_k}{k} - \frac{\partial f_p}{\partial p_\perp}\int f_k \bar{f}_k + \left(w\frac{\partial f_p}{\partial p_\perp} - \tilde{w}\frac{\partial f_p}{\partial p_z}\right)\int v f_k \bar{f}_k, \\
\mathcal{J}_z(\boldsymbol{p})/C &= -w f_p \bar{f}_p \int \frac{2f_k}{k} - \frac{\partial f_p}{\partial p_z}\int f_k \bar{f}_k - \left(\tilde{w}\frac{\partial f_p}{\partial p_\perp} + w\frac{\partial f_p}{\partial p_z}\right)\int v f_k \bar{f}_k.
\end{aligned} \tag{120}$$

We can simplify these expressions by defining the "master" integrals

$$I_a \equiv \int f_k \bar{f}_k, \tag{121}$$

$$I_b \equiv \int \frac{2f_k}{k}, \tag{122}$$

$$I_c \equiv \int v f_k \bar{f}_k. \tag{123}$$

Note that the I_c term does not appear in the expression for the current in the case of spherical symmetry and therefore represents a new feature of the cylindrical case.

We no longer need to make a distinction between $f_p = f(\boldsymbol{p})$ and $f_k = f(\boldsymbol{k})$, so we drop the subscripts. We also write w as p_z/p and $\tilde{w}$ as $p_\perp/p$.

Then the relevant components of the current read

$$\begin{aligned}
\mathcal{J}_\perp(\boldsymbol{p})/C &= -\frac{\partial f}{\partial p_\perp} I_a - \frac{p_\perp}{p} f\bar{f} I_b + \left(\frac{p_z}{p}\frac{\partial f}{\partial p_\perp} - \frac{p_\perp}{p}\frac{\partial f}{\partial p_z}\right) I_c, \\
\mathcal{J}_z(\boldsymbol{p})/C &= -\frac{\partial f}{\partial p_z} I_a - \frac{p_z}{p} f\bar{f} I_b - \left(\frac{p_\perp}{p}\frac{\partial f}{\partial p_\perp} + \frac{p_z}{p}\frac{\partial f}{\partial p_z}\right) I_c.
\end{aligned} \tag{124}$$

Equilibrium

In order for particle number to be conserved, the divergence of the current $\boldsymbol{\nabla}_{\boldsymbol{p}} \cdot \mathcal{J}(\boldsymbol{p})$ must vanish at equilibrium, i.e. for the relativistic Bose-Einstein distribution function

$$f_{\text{eq}}(\boldsymbol{p}) = \frac{1}{\exp\left(\frac{1}{T}(p^\alpha u_\alpha - \mu)\right) - 1}, \tag{125}$$

where the 4-velocity $u = \gamma(1, \boldsymbol{u})$ corresponds to the net flow. Again choosing coordinates such that $\boldsymbol{u}$ lies along the z-axis and expanding the 4-product, we have

$$f_{\rm eq}(p_\perp, p_z) = \frac{1}{\exp\left(\frac{\gamma}{T}\sqrt{p_\perp^2 + p_z^2} + \frac{\gamma u}{T}p_z - \frac{\mu}{T}\right) - 1}. \tag{126}$$

For the remainder of this section it is understood that f refers to $f_{\rm eq}$, and we will frequently drop the subscript.

Now the partial derivatives of $f_{\rm eq}$ are

$$\begin{aligned}\frac{\partial f_{\rm eq}}{\partial p_\perp} &= -\frac{\gamma}{T}\frac{p_\perp}{\sqrt{p_\perp^2 + p_z^2}}\frac{\exp\left(\frac{\gamma}{T}\sqrt{p_\perp^2 + p_z^2} + \frac{\gamma u}{T}p_z - \frac{\mu}{T}\right)}{\left(\exp\left(\frac{\gamma}{T}\sqrt{p_\perp^2 + p_z^2} + \frac{\gamma u}{T}p_z - \frac{\mu}{T}\right) - 1\right)^2} \\ &= -\frac{\gamma}{T}\frac{p_\perp}{p} f\bar{f},\end{aligned} \tag{127}$$

and

$$\begin{aligned}\frac{\partial f_{eq}}{\partial p_z} &= -\frac{\gamma}{T}\left(\frac{p_z}{\sqrt{p_\perp^2 + p_z^2}} + u\right)\frac{\exp\left(\frac{\gamma}{T}\sqrt{p_\perp^2 + p_z^2} + \frac{\gamma u}{T}p_z - \frac{\mu}{T}\right)}{\left(\exp\left(\frac{\gamma}{T}\sqrt{p_\perp^2 + p_z^2} + \frac{\gamma u}{T}p_z - \frac{\mu}{T}\right) - 1\right)^2} \\ &= -\frac{\gamma}{T}\left(\frac{p_z}{p} + u\right) f\bar{f}.\end{aligned} \tag{128}$$

We can somewhat simplify the expressions (124) for the current at equilibrium,

$$\begin{aligned}\mathcal{J}_\perp(f_{\rm eq})/C &= -\frac{\partial f}{\partial p_\perp} I_a - \frac{p_\perp}{p} f\bar{f} I_b + \left(\frac{p_z}{p}\frac{\partial f}{\partial p_\perp} - \frac{p_\perp}{p}\frac{\partial f}{\partial p_z}\right) I_c \\ &= \frac{\gamma}{T}\frac{p_\perp}{p} f\bar{f} I_a - \frac{p_\perp}{p} f\bar{f} I_b + \left(-\frac{\gamma}{T}\frac{p_z p_\perp}{p^2} f\bar{f} + \frac{\gamma}{T}\frac{p_z p_\perp}{p^2} f\bar{f} + \frac{\gamma u}{T}\frac{p_\perp}{p} f\bar{f}\right) I_c \\ &= \frac{p_\perp}{p} f\bar{f}\left(\frac{\gamma}{T} I_a - I_b + \frac{\gamma u}{T} I_c\right),\end{aligned} \tag{129}$$

and

$$\begin{aligned}\mathcal{J}_z(f_{\rm eq})/C &= -\frac{\partial f}{\partial p_z} I_a - \frac{p_z}{p} f\bar{f} I_b - \left(\frac{p_\perp}{p}\frac{\partial f}{\partial p_\perp} + \frac{p_z}{p}\frac{\partial f}{\partial p_z}\right) I_c \\ &= \frac{\gamma}{T}\left(\frac{p_z}{p} + u\right) f\bar{f} I_a - \frac{p_z}{p} f\bar{f} I_b + \left(\frac{\gamma}{T}\frac{p_\perp^2}{p^2} f\bar{f} + \frac{\gamma}{T}\frac{p_z^2}{p^2} f\bar{f} + \frac{\gamma u}{T}\frac{p_z}{p} f\bar{f}\right) I_c \\ &= \frac{p_z}{p} f\bar{f}\left(\frac{\gamma}{T} I_a - I_b + \frac{\gamma u}{T} I_c\right) + f\bar{f}\left(\frac{\gamma u}{T} I_a + \frac{\gamma}{T} I_c\right).\end{aligned} \tag{130}$$

As a sanity check, we confirm that the equilibrium current reduces to the correct form when the distribution function is spherically symmetric, $f \to f_{\rm sp}$. Given spherical symmetry, $u = 0$, $\gamma = 1$ and $I_c = \int \frac{k_z}{k} f\bar{f}$ reduces to an odd function integrated over symmetric limits and vanishes. Then

$$\begin{aligned}\mathcal{J}_r(f_{\rm sp}) &= \sqrt{\mathcal{J}_\perp(f_{\rm sp})^2 + \mathcal{J}_z(f_{\rm sp})^2} \\ &= \sqrt{\frac{p_\perp^2}{p^2}\left(f\bar{f}\left(\frac{1}{T} I_a - I_b\right)\right)^2 + \frac{p_z^2}{p^2}\left(f\bar{f}\left(\frac{1}{T} I_a - I_b\right)\right)^2} \\ &= f\bar{f}\left(\frac{1}{T} I_a - I_b\right),\end{aligned} \tag{131}$$

as required, c.f. (100).

We further confirm using Eq. (129) and (130) that the divergence of the cylindrically-symmetric current vanishes at equilibrium,

$$\boldsymbol{\nabla}_{\boldsymbol{p}} \cdot \mathcal{J}(\boldsymbol{p}) = \frac{1}{p_\perp} \frac{\partial (p_\perp \mathcal{J}_\perp)}{\partial p_\perp} + \frac{\partial \mathcal{J}_z}{\partial p_z} \stackrel{!}{=} 0. \tag{132}$$

As it turns out, the equilibrium current $\mathcal{J}$ actually vanishes identically. We obtain analytic expressions for the I_a, I_b and I_c integrals at equilibrium,

$$\begin{aligned} I_a &= 8\pi\gamma T^3 \operatorname{Li}_2\left(e^{\frac{\mu}{T}}\right), \\ I_b &= 8\pi T^2 \operatorname{Li}_2\left(e^{\frac{\mu}{T}}\right), \\ I_c &= 8\pi\gamma u T^3 \operatorname{Li}_2\left(e^{\frac{\mu}{T}}\right). \end{aligned} \tag{133}$$

By inspection we see that $I_c = -uI_a$ and $I_a = \gamma T I_b$; hence both current components (129) and (130) vanish identically.

4 Implementation

4.1 Spherical symmetry

We will detail several schemes which can be used to numerically solve the evolution equation. Using finite differences it has been possible to describe the evolution of the system up to but not including condensate formation [1]. We develop a flux-conservative scheme (the method of 'B-lines') which we will argue allows analysis of the formation of the condensate. We will also compare our findings to results from the relaxation-time approximation scheme.

Finite Differences

A straightforward application of finite differences suffices to solve the transport equation numerically, and is likely similar to the scheme used in [1]. For purposes of comparison with our method of B-lines we will briefly outline this scheme.

Writing (96) as $\frac{\partial f}{\partial \tau} = g(p, \tau)$, we can discretize time and momentum and use the forward Euler method for time,

$$f_i^{\tau+\Delta\tau} = f_i^{\tau} + \Delta\tau g(p, \tau), \tag{134}$$

and second order central differences for the momentum (with the exception of the boundary points)

$$\begin{aligned} \frac{\partial f_i^\tau}{\partial p} &= \frac{f_{i+1}^\tau - f_{i-1}^\tau}{2\Delta p}, \\ \frac{\partial^2 f_i^\tau}{\partial p^2} &= \frac{f_{i+1}^\tau - 2f_i^\tau + f_{i-1}^\tau}{\Delta p^2}. \end{aligned} \tag{135}$$

At the left endpoint we use second order forward differences,

$$\begin{aligned} \frac{\partial f_0^\tau}{\partial p} &= \frac{-3f_0^\tau + 4f_1^\tau - f_2^\tau}{2\Delta p}, \\ \frac{\partial^2 f_0^\tau}{\partial p^2} &= \frac{2f_0^\tau - 5f_1^\tau + 4f_2^\tau - f_3^\tau}{\Delta p^2}. \end{aligned} \tag{136}$$

Similarly at the right endpoint,

$$\begin{aligned} \frac{\partial f_N^\tau}{\partial p} &= \frac{3f_N^\tau - 4f_{N-1}^\tau + f_{N-2}^\tau}{2\Delta p}, \\ \frac{\partial^2 f_N^\tau}{\partial p^2} &= \frac{2f_N^\tau - 5f_{N-1}^\tau + 4f_{N-2}^\tau - f_{N-3}^\tau}{\Delta p^2}. \end{aligned} \tag{137}$$

The primary disadvantage of this scheme is that it requires a high-resolution discretization of momentum space. This becomes particulary problematic when generalizing to situations without spherical symmetry ("full degrees of freedom"); the so-called "curse of dimensionality" results in a computationally challenging number of variables.

We will therefore put forward a more computationally efficient scheme, the form of which expresses the underlying physics of the system manifestly.

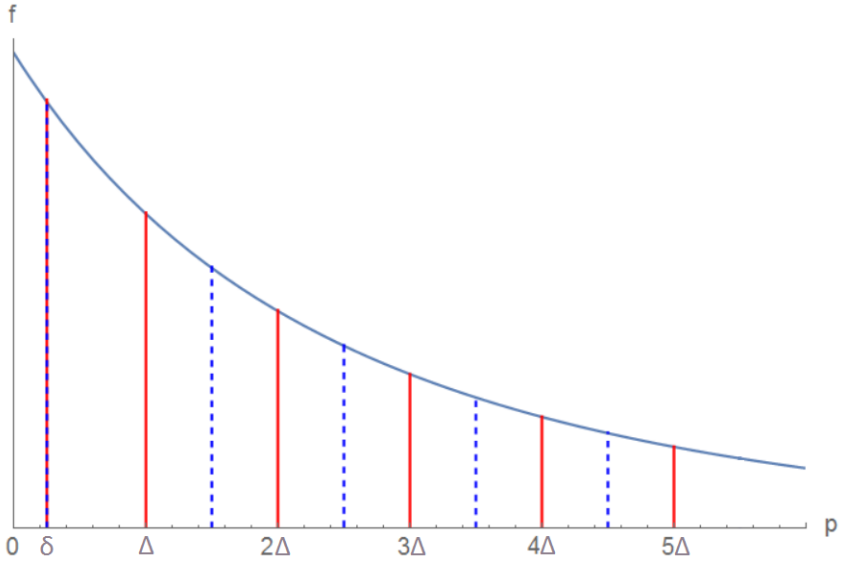

Figure 4: The "method of b-lines" scheme, illustrated for the spherically symmetric case. Solid red lines denote the gridpoints p_i of the interpolation. Dashed blue lines represent the boundaries between cells. See text for details.

The Method of 'B-lines'

Our method of 'B-lines' is a flux-conservative numerical scheme which we have developed in order to solve the Boltzmann equation. The name is a reference to the well known Method of Lines [22], with the 'B' referring to an efficient parameterization of the distribution function in terms of piecewise Bose functions. We illustrate it in figure 4.

Starting from the initial spherically symmetric distribution function, we discretize the momentum grid into bins of width Δ and construct a piecewise approximation of f. As mentioned, instead of a piecewise linear interpolation, we employ a set of M piecewise Bose distribution functions which we

call 'B-lines',

$$f^{(i)}(p) = \frac{1}{e^{a_i p + b_i} - 1}, \tag{138}$$

where a_i and b_i are parameters of the interpolation. The domain of $f^{(i)}$ is $p \in [i, (i+1)]\Delta$ for $0 \leq i < M-1$ and $[\Delta(M-1), \infty)$ for $i = M-1$.

A couple of points are in order. Firstly, it should be noted that this choice is equivalent to a linear interpolation of a particular transformation of the distribution function, $g \equiv \ln(\bar{f}/f)$, i.e.

$$g^{(i)}(p) = a_i p + b_i. \tag{139}$$

One of the reasons that we choose to make this transformation is that Bose distributions corresponding to overpopulated initial conditions are singular at $p = 0$, which would make linear interpolation impossible. The function g conveniently goes to zero instead.

Secondly, for an equilibrium distribution function, our interpolation scheme is actually exact, which is a nice property. An equilibrium distribution in g-space of course is simply a straight line.

Physically, the a_i correspond to local inverse temperature parameters, and the b_i correspond to the chemical potential. We determine them initially by sampling the distribution function at gridpoints illustrated in Fig. 4,

$$\begin{aligned} f_0 &\equiv f(\delta), \\ f_i &\equiv f(\Delta i), \;\; 0 < i < M. \end{aligned} \tag{140}$$

Here δ is small relative to Δ but non-zero in order to avoid singularities at the origin.

We can then use the usual formulae for linear interpolation, recalling that the function we are interpolating is $g \equiv \ln\left(\frac{\bar{f}}{f}\right)$. After some algebra we obtain

$$\begin{aligned} a_0 &= \frac{1}{\Delta - \delta} \ln\left(\frac{\bar{f}_1 f_0}{f_1 \bar{f}_0}\right), \\ b_0 &= \ln\left(\frac{\bar{f}_1}{f_1}\right) - \Delta a_0, \\ a_i &= \frac{1}{\Delta} \ln\left(\frac{\bar{f}_i f_{i-1}}{f_i \bar{f}_{i-1}}\right), \;\; 0 < i < M, \\ b_i &= \ln\left(\frac{\bar{f}_1}{f_1}\right) - i\Delta a_i, \;\; 0 < i < M. \end{aligned} \tag{141}$$

Having established the details of the initial interpolation, we now consider the process by which we evolve the distribution function in time.

As per figure 4, we divide the p-axis into $M + 1$ cells, separated at the momenta

$$\begin{aligned} p_0 &= \delta, \\ p_i &= \left(i + \frac{1}{2}\right)\Delta, \;\; 0 < i < M. \end{aligned} \tag{142}$$

such that cell 0 is $[0, \delta]$, cell M is $[(M - \frac{1}{2})\Delta, \infty)$ and an intermediate cell with $0 < i < M$ is $[p_{i-1}, p_i]$.

This discretization is "staggered" with respect to the grid used for the interpolation, with the distribution function in each cell being interpolated by two B-lines. This is because as we will see shortly, the first derivative of our interpolation of the distribution function is required to be continuous at our cell boundaries, which is not in general the case at B-line boundaries.

From the B-lines we can calculate the total particle number (per volume) in each cell,

$$\begin{aligned} n_0 &= \frac{4\pi}{(2\pi)^3}\int_0^{\delta} \mathrm{d}p\, p^2 f^{(0)}(p), \\ n_i &= \frac{4\pi}{(2\pi)^3}\int_{p_{i-1}}^{\Delta i} \mathrm{d}p\, p^2 f^{(i-1)}(p) + \frac{4\pi}{(2\pi)^3}\int_{\Delta i}^{p_i} \mathrm{d}p\, p^2 f^{(i)}(p), \quad 0 < i < M, \\ n_M &= \frac{4\pi}{(2\pi)^3}\int_{p_{M-1}}^{\infty} \mathrm{d}p\, p^2 f^{(M-1)}(p). \end{aligned} \tag{143}$$

These integrals can be solved analytically. In general,

$$\begin{aligned} n(p_1, p_2, a, b) &\equiv \frac{4\pi}{(2\pi)^3}\int_{p_1}^{p_2} \mathrm{d}p\, p^2 \frac{1}{e^{ap+b}-1} \\ &= \frac{1}{2a^3\pi^2}\Bigg[a^2\Bigg(p_1^2(ap_1+b) - bp_2^2 - ap_2^3 - p_1^2 \ln\left(e^{ap_1+b}-1\right) \\ &\quad + p_2^2 \ln\left(e^{ap_2+b}-1\right)\Bigg) + 2ap_1 \operatorname{Li}_2\left(e^{-(ap_1+b)}\right) - 2ap_2 \operatorname{Li}_2\left(e^{-(ap_2+b)}\right) \\ &\quad + 2\operatorname{Li}_3\left(e^{-(ap_1+b)}\right) - 2\operatorname{Li}_3\left(e^{-(ap_2+b)}\right)\Bigg]. \end{aligned} \tag{144}$$

By expressing the a_i and b_i parameters in terms of the f_i using (141) we find

we have expressions for the particle number density in the $M+1$ cells in terms of the $M+1$ f_i parameters. For the sake of brevity we will not write down the full set of expressions here. Additionally, we can find similarly lengthy, but closed form solutions to the I_a, I_b integrals which we also omit.

Now, recall that the Fokker-Planck equation can be written as a continuity equation (conserving both particle number and energy), as in (97). Thus the rate of change of particle number in cell i,

$$\dot{n_i} = \partial_\tau \frac{4\pi}{(2\pi)^3} \int_{p_i}^{p_{i+1}} \mathrm{d}p p^2 f(p,\tau) = \frac{4\pi}{(2\pi)^3} p^2 \mathcal{J}(p) \Big|_{p_i}^{p_{i+1}} \tag{145}$$

is given by $\phi_{i+1} - \phi_i$, the net flux into cell i, which is determined by the flux through the respective spherical surfaces,

$$\phi_i \equiv \frac{4\pi}{(2\pi)^3} p^2 \mathcal{J}(p_i) = \frac{4\pi}{(2\pi)^3} p^2 (I_a \partial_p f + I_b f(1+f)) \Big|_{p=p_i}. \tag{146}$$

Note that the zeroth cell is exceptional. The flux at $p = 0$ (ϕ_0) is 0 by construction. Similarly, the last cell's rightmost boundary is at infinity, with zero flux through it.

We thus arrive at the following non-linear system of ODEs,

$$\begin{aligned} \dot{n}_0 &= \phi(\delta), \\ \dot{n}_i &= \phi_{i+1} - \phi_i, \;\; 0 < i < M, \\ \dot{n}_M &= -\phi_M. \end{aligned} \tag{147}$$

Note that the integrals I_a and I_b, which determine the flux according to (146)

depend on all of the f_i and must be updated at each time step.

We can solve these ODEs using the forward Euler method. Having updated the particle number in each cell, it is straightforward to find the evolved set of B-line parameters.

One advantage of the modified scheme is that it allows us to compute the number of particles in the condensate. Analysis shows that the flux into the zeroth cell[2] becomes non-zero after finite time for overpopulated systems approaching the equilibrium Bose-Einstein distribution. However in the high-time limit, the flux becomes proportional to $I_b - \frac{1}{T} I_a$. For an equilibrium distribution, this term vanishes. The distribution function in the zeroth cell can be obtained by extrapolation, and the particle number thereby obtained. We will see that this number exceeds the number of particles predicted by the equilibrium distribution in the overpopulated case. We argue that the difference in particle number is precisely the number of particles scattered into the condensate.

4.2 Cylindrical symmetry

We can generalize the "method of B-lines" algorithm to solve for initial conditions with cylindrical symmetry – i.e. with "one more degree of freedom" than the spherically symmetric case. In this case, rather than interpolating a curve, we are interpolating a 2D surface.

The initial challenge is to construct a grid over the momentum space, dividing it into cells covered by a piecewise function that interpolates the arbitrary

[2]Note that this flux remains well-defined as we take the limit $\delta \to 0$.

initial condition. We would like this grid to have the following properties.

- The piecewise interpolation should occur over triangular 'tiles' defined by three non-collinear gridpoints.
- The number of cells must be equal to the number of gridpoints (+1 for the condensate) in order for the system to be closed.
- The boundaries of the cells and the boundaries of the interpolation tiles may intersect but must not coincide, as we require the gradient of the interpolation function over the cell boundaries to be well-defined.

While cylindrical coordinates are a natural choice given the symmetry of the problem, we propose a modified coordinate system in which the p_T coordinate is replaced by the energy $\omega \equiv \sqrt{p_T^2 + p_z^2}$, as it meets these requirements very elegantly. Firstly, it is geometrically convenient. Since $|p_z|$ cannot exceed ω, the ω-p_z half-plane is restricted by the lines $\omega = \pm p_z$ to a triangular subspace that can easily be partitioned into triangular interpolation tiles. Secondly, recall that the equilibrium Bose distribution for a cylindrically symmetric (or, choosing the z-axis to coincide with $\boldsymbol{u}$, an arbitrary) initial condition is of the form

$$f_B = \frac{1}{e^{g(p_z,p_T)} - 1} \tag{148}$$

where

$$g(p_z, p_T) = \frac{\gamma}{T}\sqrt{p_z^2 + p_T^2} + \frac{\gamma u}{T}p_z - \frac{\mu}{T} \tag{149}$$

is an expression that is nonlinear in terms of p_z, p_T but linear in terms of p_z, ω,

$$g(p_z, \omega) = \frac{\gamma}{T}\omega + \frac{\gamma u}{T}p_z - \frac{\mu}{T}, \tag{150}$$

which simplifies various integrals and also allows us to consider interpolating the distribution function f with Bose functions f_i as performing a simple linear interpolation of the function $\ln\left(\bar{f}/f\right)$ with planar functions g_i. We will discuss the details of this below.

We therefore construct the following scheme (see Fig. 5).

Define unit vectors $\hat{e}_1 = \frac{1}{\sqrt{2}}\left(\hat{\omega} - \hat{p}_z\right)$ and $\hat{e}_1 = \frac{1}{\sqrt{2}}\left(\hat{\omega} + \hat{p}_z\right)$. For an n-level grid with some specified grid spacing Δ, we place gridpoints at points $(i\Delta, j\Delta)$ in the $\hat{e}_1 - \hat{e}_2$ basis with $i, j \in \mathbb{N}$ and $i + j \leq n$. However, to avoid the singular value at the origin at equilibrium we shift the $(0, 0)$ point in the $\hat{w}$ direction by a distance $\delta \ll \Delta$.

The triangular tiles for the interpolation are defined by simply connecting nearest neighbours in a hexagonal grid. The midpoints of the tile boundaries then define a square grid with gridpoints at the centre of each square. This grid forms the boundaries of the particle number cells, in analogy with the "staggered grid" of the spherically symmetric scheme.

Step by step, the algorithm is as follows.

First, from the initial distribution function, find the B-line for each tile. This amounts to simultaneously solving the equations

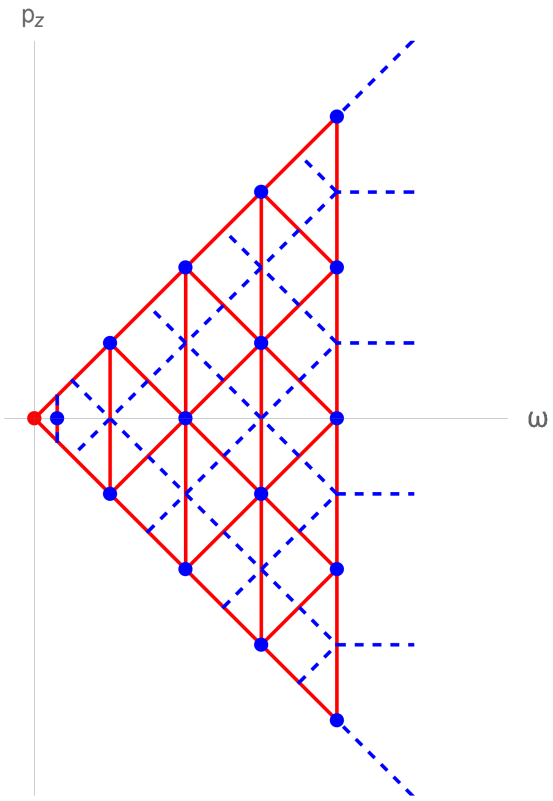

Figure 5: Illustrating the scheme for cylindrically symmetric distributions. In analogy with figure 4, solid (red) lines indicate the boundaries of the piecewise interpolation. Dashed (blue) lines indicate the boundaries of the cells.

$$\begin{aligned} \frac{1}{e^{a\omega_i + bp_{z,i} + c}} &= f_i, \;\; i = 1, 2, 3 \\ \implies a\omega_i + bp_{z,i} + c &= \ln\left(\frac{1+f_i}{f_i}\right), \end{aligned} \tag{151}$$

which is just a linear plane interpolation with solution

$$a = \frac{(p_{z,2} - p_{z,3}) \ln\left(\frac{\bar{f}_1}{f_1}\right) + (-p_{z,1} + p_{z,3}) \ln\left(\frac{\bar{f}_2}{f_2}\right) + (p_{z,1} - p_{z,2}) \ln\left(\frac{\bar{f}_3}{f_3}\right)}{\omega_1(p_{z,2} - p_{z,3}) + \omega_2(-p_{z,1} + p_{z,3}) + \omega_3(p_{z,1} - p_{z,2})},$$

$$b = \frac{(\omega_2 - \omega_3) \ln\left(\frac{\bar{f}_1}{f_1}\right) + (-\omega_1 + \omega_3) \ln\left(\frac{\bar{f}_2}{f_2}\right) + (\omega_1 - \omega_2) \ln\left(\frac{\bar{f}_3}{f_3}\right)}{p_{z,1}(\omega_2 - \omega_3) + p_{z,2}(-\omega_1 + \omega_3) + p_{z,3}(\omega_1 - \omega_2)},$$

$$c = \frac{(\omega_2 p_{z,3} - \omega_3 p_{z,2}) \ln\left(\frac{\bar{f}_1}{f_1}\right) + (\omega_3 p_{z,1} - \omega_1 p_{z,3}) \ln\left(\frac{\bar{f}_2}{f_2}\right) + (\omega_1 p_{z,2} - \omega_2 p_{z,1}) \ln\left(\frac{\bar{f}_3}{f_3}\right)}{\omega_1(p_{z,2} - p_{z,3}) + \omega_2(-p_{z,1} + p_{z,3}) + \omega_3(p_{z,1} - p_{z,2})}. \tag{152}$$

For the first iteration it is also necessary to calculate the particle number in each cell via numerical integration, as well as I_a, I_b and I_c.

Next, calculate the flux into each cell and update the particle number accordingly. Recall that the particle current for a Bose distribution (making the substitutions $\frac{\gamma}{T} \to a$, $\frac{\gamma u}{T} \to b$ and $-\frac{\mu}{T} \to c$) is given by

$$\begin{aligned} \mathcal{J}_\perp(f_{\text{eq}})/C &= \frac{p_\perp}{p} f\bar{f}\,(aI_a - I_b + bI_c) \\ \mathcal{J}_z(f_{\text{eq}})/C &= \frac{p_z}{p} f\bar{f}\,(aI_a - I_b + bI_c) + f\bar{f}\,(bI_a + aI_c) \end{aligned} \tag{153}$$

For this step cylindrical coordinates were used; the surfaces of the cells in 3D therefore corresponded to sections of spheres and paraboloids. It is of course also possible to calculate the current in the ω-p_z coordinates in which case the integration would be performed over rings and cone sections.

From the updated particle numbers, we update the piecewise interpolation of the distribution function. This amounts to solving the system of $n + 1$ coupled algebraic equations (where n is the number of gridpoints) equating the analytical expressions for the particle number in each cell (in terms of the a_i, b_i, c_i parameters).

The cells are covered by the interpolation tiles in a non-uniform way, but it is for instance possible to break them up into right-angled triangles that fall within only one interpolation tile.

The above steps are then repeated until equilibrium is reached.

4.3 Relaxation Time Approximation

An alternative, crude approximation to the Boltzmann equation is the Relaxation Time Approximation. Also known as the BGK (Bhatnagar, Gross and Kook) approximation [17], it takes the form of an ansatz for the collision term. For the non-relativistic Boltzmann equation,

$$C_{[f]}^{BGK} = \frac{f_\infty - f}{\tau}, \tag{154}$$

where f_∞ is the equilibrium distribution function and the eponymous relaxation time τ is a parameter that controls the rate of approach to equilibrium.

It can be thought of as an "averaged" value of the actual collision term.

For our purposes we will require the manifestly covariant generalization of the BGK equation (due to Anderson and Witting [23]),

$$p^\mu \partial_\mu f = p^\mu u_\mu \frac{f_\infty - f}{\tau}, \tag{155}$$

where u_μ is the collective flow velocity.

For a spatially homogeneous system, $p^\mu \partial_\mu \to p_0 \partial_t$, so we have

$$\partial_t f = \frac{p^\mu u_\mu}{p_0} \frac{f_\infty - f}{\tau}, \tag{156}$$

which is a simple separable differential equation with the analytic solution

$$f(t) = f_\infty + (f_0 - f_\infty) e^{-\left(\frac{p^\mu u_\mu}{p_0} \frac{t}{\tau}\right)}. \tag{157}$$

While spatially inhomogeneous systems are for the most part beyond the scope of this thesis, there are interesting dynamics that emerge from the RTA in that more general case that we will discuss briefly. In particular, for certain numerical schemes it becomes necessary to solve the RTA in locally spatially homogeneous cells with variable particle number due to streaming and consequently variable local f_∞.

Discretizing (157), we derive the update equation

$$f(t + \Delta t) = f_\infty + (f(t) - f_\infty) e^{-\left(\frac{p^\mu u_\mu}{p_0} \frac{\Delta t}{\tau}\right)}. \tag{158}$$

Note that if we expand the exponential in a Taylor series to first order in Δt we recover the forward Euler method,

$$\begin{aligned} f(t+\Delta t) &= f_\infty + (f(t) - f_\infty)\left(1 - \frac{p^\mu u_\mu}{p_0}\frac{\Delta t}{\tau}\right) \\ &= f(t) + \frac{p^\mu u_\mu}{p_0}\frac{f_\infty - f(t)}{\tau}\Delta t. \end{aligned} \tag{159}$$

Now, in order to update the equilibrium distribution f_∞ with each time step, we take advantage of energy-momentum conservation as follows.

Recall that the energy-momentum tensor is defined as

$$T^{\mu\nu} \equiv \int \frac{p^\mu p^\nu}{p^0} f. \tag{160}$$

Energy-momentum conservation is conveniently represented in covariant form as

$$\partial_\mu T^{\mu\nu} = \partial_\mu \int \frac{p^\mu p^\nu}{p^0} f = \int \frac{p^\nu}{p^0}\left(p^\mu \partial_\mu f\right) \stackrel{!}{=} 0. \tag{161}$$

Substituting (155) into (161), we have

$$\begin{aligned} 0 &= \int \frac{p^\nu}{p^0}\left(p^\mu u_\mu \frac{f_{eq} - f}{\tau}\right) \\ &= u_\mu \int \frac{p^\mu p^\nu}{p^0}\left(f_{eq} - f\right) \\ &= u_\mu \left[T^{\mu\nu}_{[f_{eq}]} - T^{\mu\nu}_{[f]}\right]. \end{aligned} \tag{162}$$

Now, for an ideal fluid in equilibrium,

$$T^{\mu\nu}_{LRF} = (\epsilon + P)u^\mu u^\nu - P g^{\mu\nu}, \tag{163}$$

where ϵ and P are the LRF energy density and pressure respectively. Thus

$$\begin{aligned} u_\mu T^{\mu\nu}_{[f_{eq}]} &= (\epsilon + P)(u_\mu u^\mu)u^\nu - P u_\mu g^{\mu\nu} \\ &= \epsilon u^\nu. \end{aligned} \tag{164}$$

Further,

$$\begin{aligned} u_\mu T^{\mu\nu} &= u_\mu T^{\nu\mu} \\ &= u^\alpha g_{\alpha\mu} T^{\nu\mu} \\ &= u^\alpha T^\nu{}_\alpha \\ &= T^\nu{}_\mu u^\mu, \end{aligned} \tag{165}$$

where in the first step we have taken advantage of the symmetric nature of $T^\mu\nu$ to swap indices and relabeled the dummy index α.

Altogether we have the eigenvalue equation

$$T^\nu{}_\mu u^\mu = \epsilon_{eq} u^\nu, \tag{166}$$

which we can solve for u^μ and ϵ_{eq}.

Recall that Lorentz transformations do not change the eigenvalues of T^ν_μ. Further, from our energy-momentum conservation condition Eq. (162), we

know that the eigenvalues are the same as for the equilibrium distribution. As the matrix representation is diagonal in the rest frame at equilibrium, we can read off the eigenvalues as ϵ, $-P_1$, $-P_2$, $-P_3$, of which only one will be positive. Correspondingly, there will be only one time-like eigenvector. We can therefore be confident that there is no ambiguity in solving the eigenvalue equation for ϵ_{eq}.

We arrive at a similar equation for particle number conservation, starting from

$$\begin{aligned} 0 &= \partial_\mu J^\mu \\ &= \partial_\mu \int p^\mu f \quad = \int p^\mu \partial_\mu f = \int p^\mu u_\mu \frac{f_{eq} - f}{\tau} \quad = u_\mu \left[J^\mu_{eq} - J^\mu \right]. \end{aligned} \tag{167}$$

J^μ_{eq} of course is just $n_{eq} u^\mu$, so

$$\begin{aligned} u_\mu J^\mu &= u_\mu J^\mu_{eq} \\ &= n_{eq}(u_\mu u^\mu) \\ &= n_{eq}. \end{aligned} \tag{168}$$

Thus by finding $T^{\mu\nu}$ and J^μ at time t we can obtain the corresponding equilibrium energy and number densities and hence obtain the parameters of the equilibrium Bose distribution. These can be updated with each timestep, as is necessary in schemes with particle streaming into cells. This results in a "running" equilibrium.

5 Results

We present a selection of results, starting with spherically symmetric initial conditions before generalizing to cylindrical symmetry. The small-scattering approximation is compared to the relaxation time approximation and used to estimate the relaxation time parameter for the initial conditions chosen. Additionally we quantify and investigate anisotropy in the initial conditions, and in particular compare isotropization time to thermalization time.

5.1 Spherically symmetric initial conditions

We consider the family of CGC-inspired initial conditions

$$f(\omega) = f_0 \frac{1}{e^{\frac{1}{T}(\omega - Q)} + 1}. \tag{169}$$

For purposes of demonstrating and comparing some representative results from our scheme, we choose $T = 0.05$ and $Q = 1$, where the small value of T produces a characteristic "sharp corner" of the momentum distribution near $p = Q$, and Q sets the momentum scale. For these values of the parameters, the distribution function becomes critically populated at $f_0 = 0.161946$.

For somewhat technical implementation purposes, it is useful to multiply the above distribution function by an overall factor of $e^{-0.01\omega}$ to avoid issues related to floating point imprecision. For this modified initial condition, the critical value of f_0 is 0.162912.

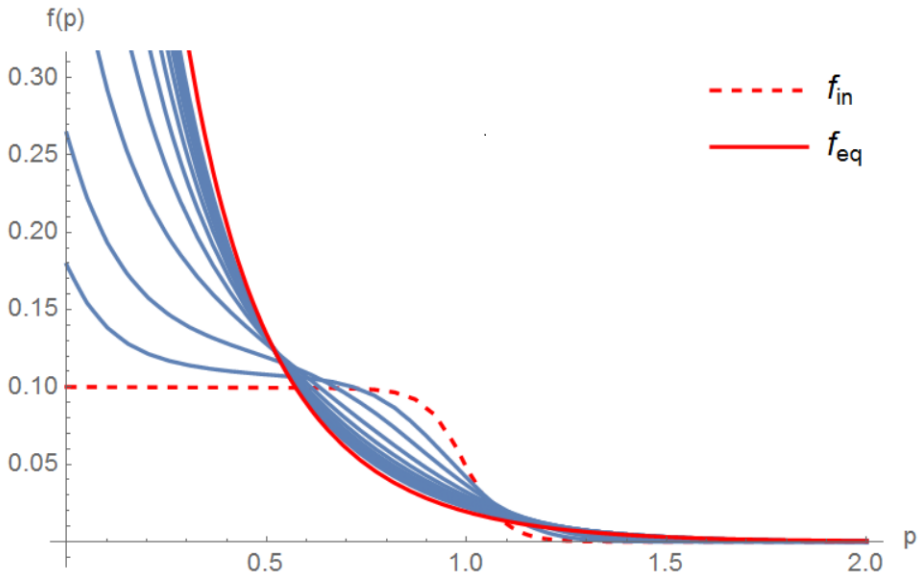

Figure 6: Evolution of the distribution function at various timesteps.

5.1.1 Underpopulated

For underpopulated initial conditions, the equilibrium distribution function has a strictly negative μ and does not become singular at the origin. Further, no condensate forms.

Figure 6 shows the evolution of a distribution function of the form of (169) with $T = 0.05$, $Q = 1$ and $f_0 = 0.1$ at various (arbitrary) intermediate timesteps. Figure 7 shows the same evolution on a logarithmic scale.

Recall that by making the transformation

$$g(p) \equiv \ln\left(\frac{1+f(p)}{f(p)}\right) \tag{170}$$

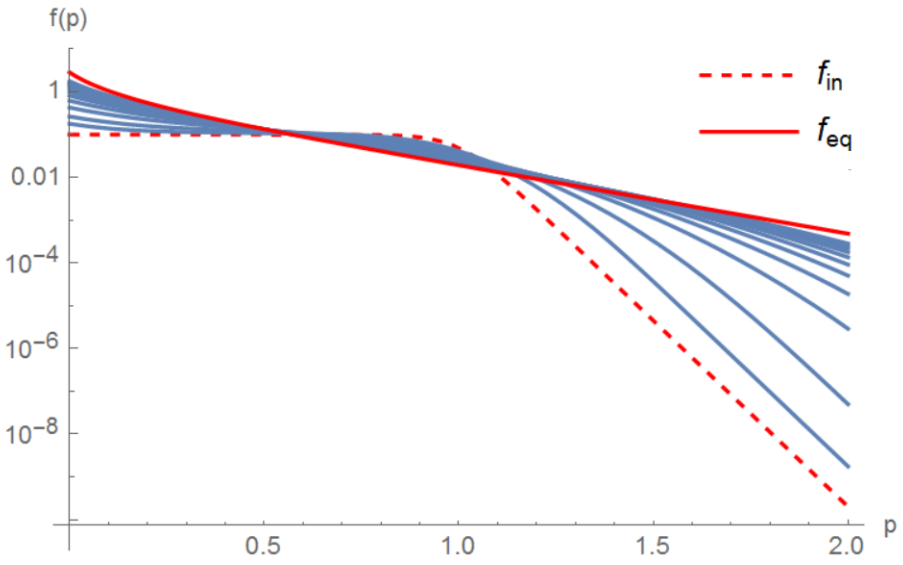

Figure 7: Same evolution shown in Fig. 6 on a logarithmic scale.

the equilibrium distribution function can be represented as a straight line. We plot the evolution in terms of $g(p)$ over time in figure 8.

Worth examining is the particle current that drives the evolution. Plotting $\mathcal{J}(p)$ alongside the distribution function (scaled down to fit) in Fig. 9, we see that the particle flow is negative at soft momenta and positive at harder momenta, indicating a flux of gluons from harder to softer modes in phase space.

5.1.2 Equilibriation time and comparison to the relaxation time approximation

As shown in Sec. 2.4.1 the entropy density of the system of gluons is a monotonically increasing function of time that will asymptotically converge

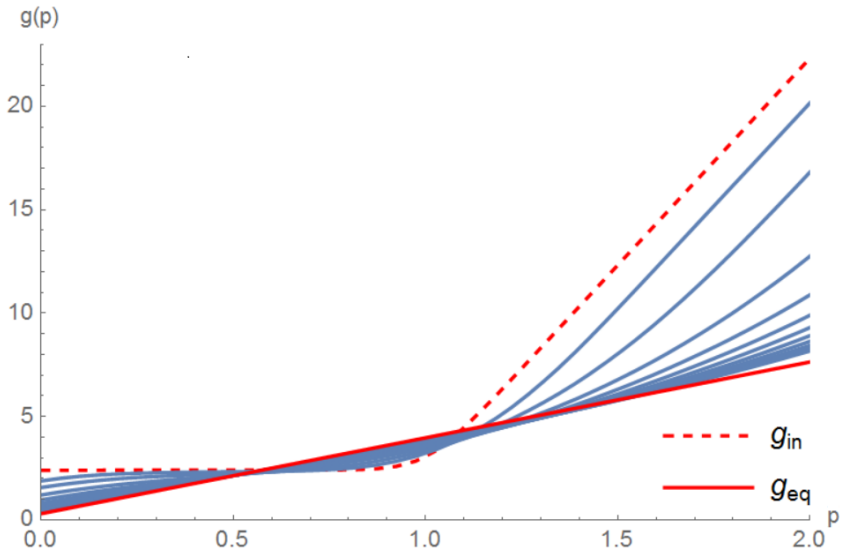

Figure 8: Same evolution as Figs. 6,7, now in terms of g after the mapping given by Eq. (170).

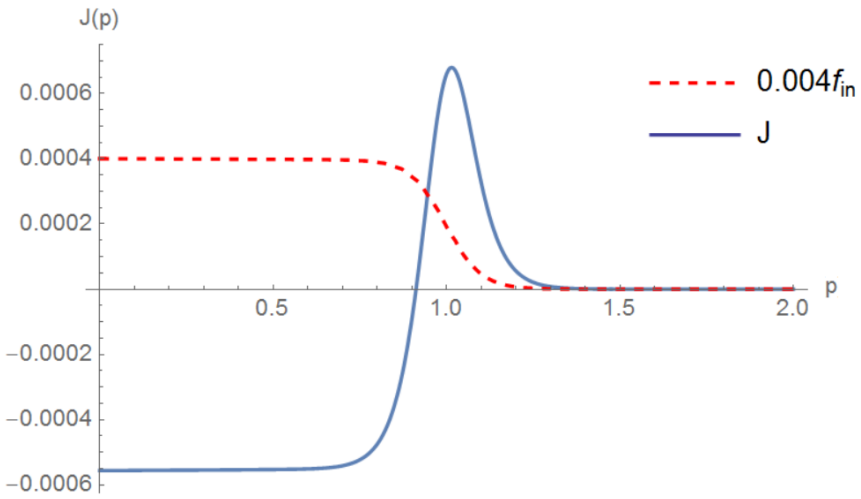

Figure 9: Particle current for the initial distribution function (shown at reduced scale).

to a fixed value. This makes it a good measure of the thermalization of the system.

However, while our numerical scheme conserves particle number exactly, due to the discretization of the momentum grid, energy is not perfectly conserved. As a result the parameters of the projected equilibrium distribution will change slightly over time.

Therefore we define the "equilibriation parameter"

$$\eta \equiv S/S_\infty, \tag{171}$$

where S is the current entropy density and S_∞ is the entropy density of the currently projected equilibrium distribution. This parameter should increase monotonically and asymptotically approach 1. Plotting this parameter for the current example in figure 10 we see that this is indeed the case, and we can read off an approximate equilibriation time.

Now, consider the relaxation time approximation. For spherically symmetric initial conditions we have an analytic solution, viz.

$$f(t) = f(\infty) + (f(0) - f(\infty))e^{-\frac{t}{\tau}}, \tag{172}$$

an exponential approach to equilibrium controlled by the relaxation time parameter τ. Note that τ is a free parameter of the model and must be specified. It is desirable to use a comparison to the small scattering approximation in order to estimate an appropriate value.

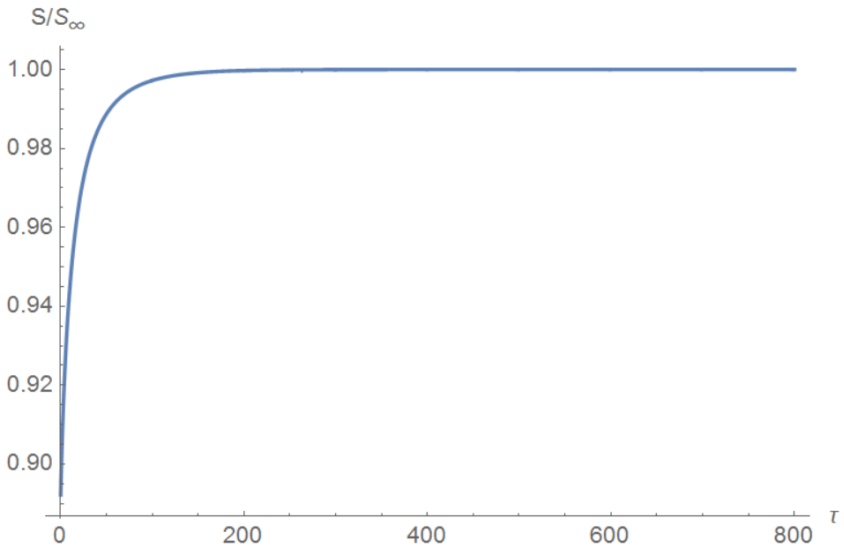

Figure 10: Evolution of the "equilibriation" parameter showing the approach to equilibrium

For a given value of p, observe that $\frac{f(p,t)}{f(p,\infty)}$ approaches 1. We wish to investigate the rate of this approach,

$$\begin{aligned} 1 - \frac{f(p,t)}{f(p,\infty)} &= 1 - (1 + f(p,0)/f(p,t) - 1)e^{-\frac{t}{\tau}} \\ &= (1 - f(p,0)/f(p,t))e^{-\frac{t}{\tau}}. \end{aligned} \tag{173}$$

Taking the logarithm, we obtain a function linear in t,

$$\ln\left(1 - \frac{f(p,t)}{f(p,\infty)}\right) = \ln(1 - f(p,0)/f(p,t)) - \frac{t}{\tau}. \tag{174}$$

Inspired by this, we do the same for the equilibriation parameter as defined in Eq. 171 (a more physically motivated measure of the approach to equilibrium

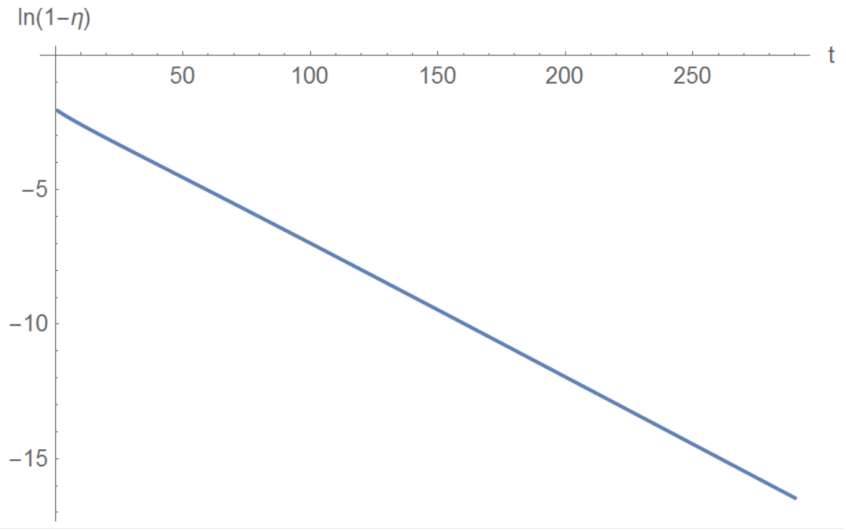

Figure 11: $\ln(1-\eta)$ evolution for RTA, showing linear behaviour.

than the value of f at some arbitrary p). Plotting $\ln(1-\eta)$ for the same initial condition in Fig. 6, we do indeed see linear behaviour (see Fig. 11).

This motivates us to consider the parameter $\ln(1-\eta)$ in the small-scattering approximation (for the same initial condition). Plotting this in figure 12, we again see linear behaviour leading up to equilibrium. Fitting a straight line to this part of the plot, we can read off an estimate for the corresponding relaxation time parameter τ for this initial condition.

Here the equation of the line of best fit is $y = -0.022779x - 3.61004$, corresponding to $\tau = 43.9$ in the units of our scheme.

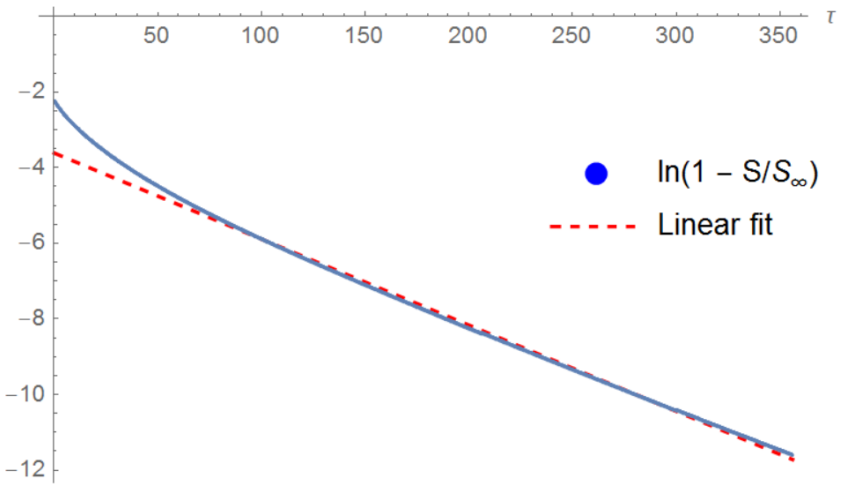

Figure 12: $\ln(1-\eta)$ evolution for method of B-lines with line of best fit

5.1.3 Overpopulated

As discussed, there exist initial conditions that have an overabundance of gluons relative to their total energy density; these overpopulated systems will evolve to a Bose-Einstein distribution function with zero chemical potential and a Bose-Einstein condensate term.

If we attempt to evolve an initial distribution function of the form of (169) with f_0 in excess of the critical value of 0.162912, e.g. $f_0 = 0.2$ using our numerical scheme without implementing the zeroth cell, i.e. with $\delta = 0$, we are able to evolve the system only to the onset of Bose-Einstein condensation and not beyond. See figure 13.

Note that the system approaches but ultimately exceeds the projected equilibrium distribution. This is as expected; the system contains an overabun-

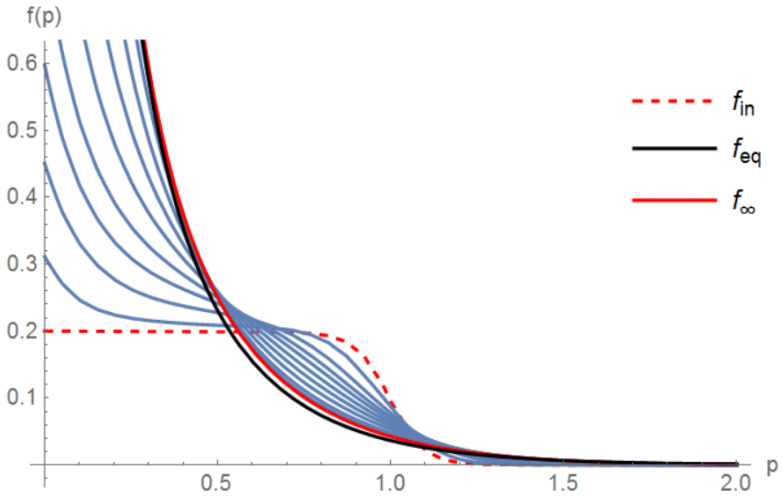

Figure 13: Evolution of the overpopulated distribution function using the scheme without the zeroth cell.

dance of gluons.

Using the scheme with the zeroth cell, however, we argue that we are able to model the inital formation of the condensate. Unfortunately the numerics break down before equilibrium is fully reached, but importantly we do manage to evolve the system beyond the onset of condensation, as well as recover some qualitative information from the partial evolution. In figures 14 and 15 we show this evolution. Note in particular that the system approaches the projected equilibrium more closely than in figure 13.

It is of course easy to evolve overpopulated initial conditions to equilibrium using the relaxation time approximation. In figure 16 we show this for the same initial conditions. We observe a qualitative difference in the formation of the condensate. Using the method of B-lines resulted in a period of very slow growth followed by a rapid spike; the relaxation time approximation has

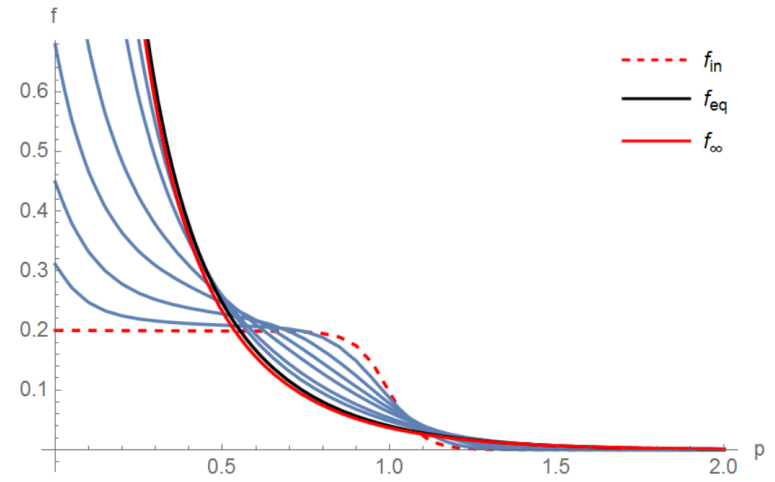

Figure 14: Evolution of the overpopulated distribution function using scheme with zeroth cell implemented.

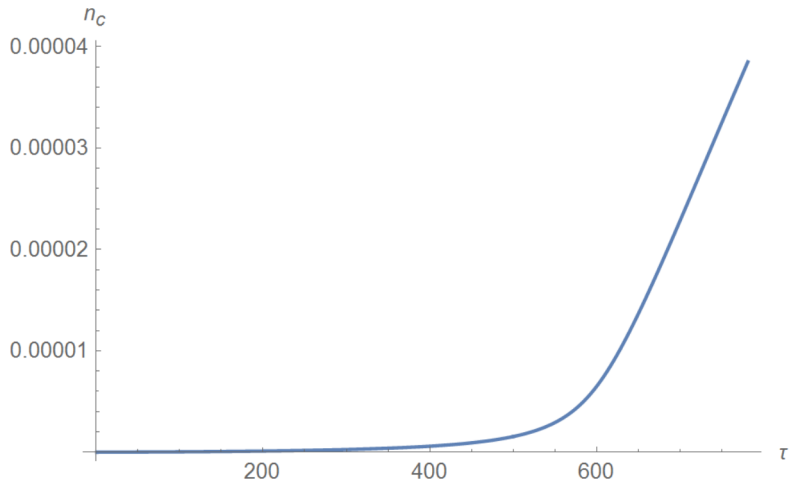

Figure 15: Evolution of the condensate corresponding to the system of figure 14, up to the point of failure of the numerical scheme.

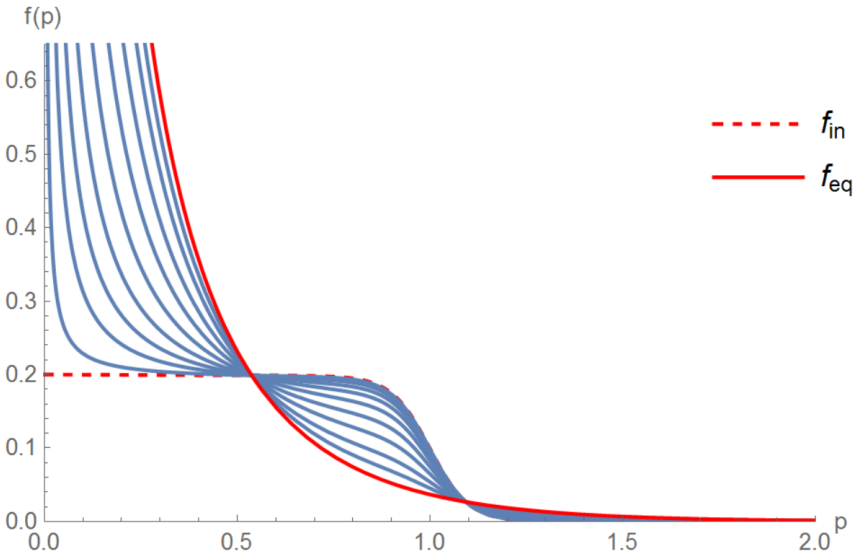

Figure 16: Evolution of the overpopulated system according to the relaxation time approximation.

steady growth from $t = 0$.

5.2 Cylindrically symmetric initial conditions

Having generalized from spherically symmetric to cylindrically symmetric initial conditions, it becomes possible to explore the effects on anisotropy on the evolution of the distribution function. It is important to differentiate between isotropic distribution functions just boosted out of their rest frame and distribution functions that are "generically" anisotropic, i.e. even in their rest frame.

In order to study anisotropy of the second kind, we follow Strickland [24] and consider initial conditions of the form

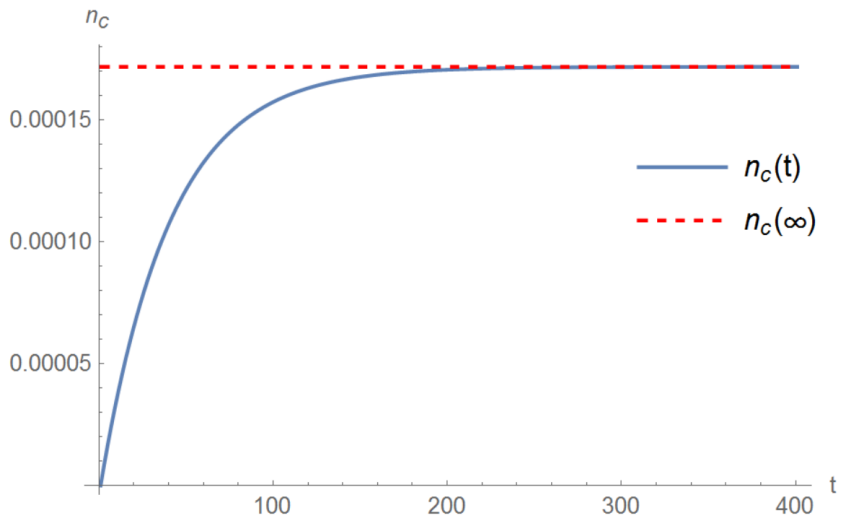

Figure 17: Evolution of the condensate according to the relaxation time approximation

$$f(\omega, p_z) \to \left(\sqrt{1+\xi}\right) f(\sqrt{\omega^2 + \xi p_z^2}, p_z), \tag{175}$$

where $\xi > -1$ governs the anisotropy and the factor of $\sqrt{1+\xi}$ is a normalization to preserve particle number and energy density.

To illustrate this, we plot a rest frame Fermi-Dirac distribution function for $\xi = -0.5$, 0 and 0.5 in figure 18.

It is easily seen that introducing ξ spreads out the particle distribution over higher z momenta for negative values of ξ, with the reverse being true for positive values.

We can generalize our spherically symmetric initial condition (169) using this anisotropization. Additionally (as we will see in Eq. (176)) we introduce a

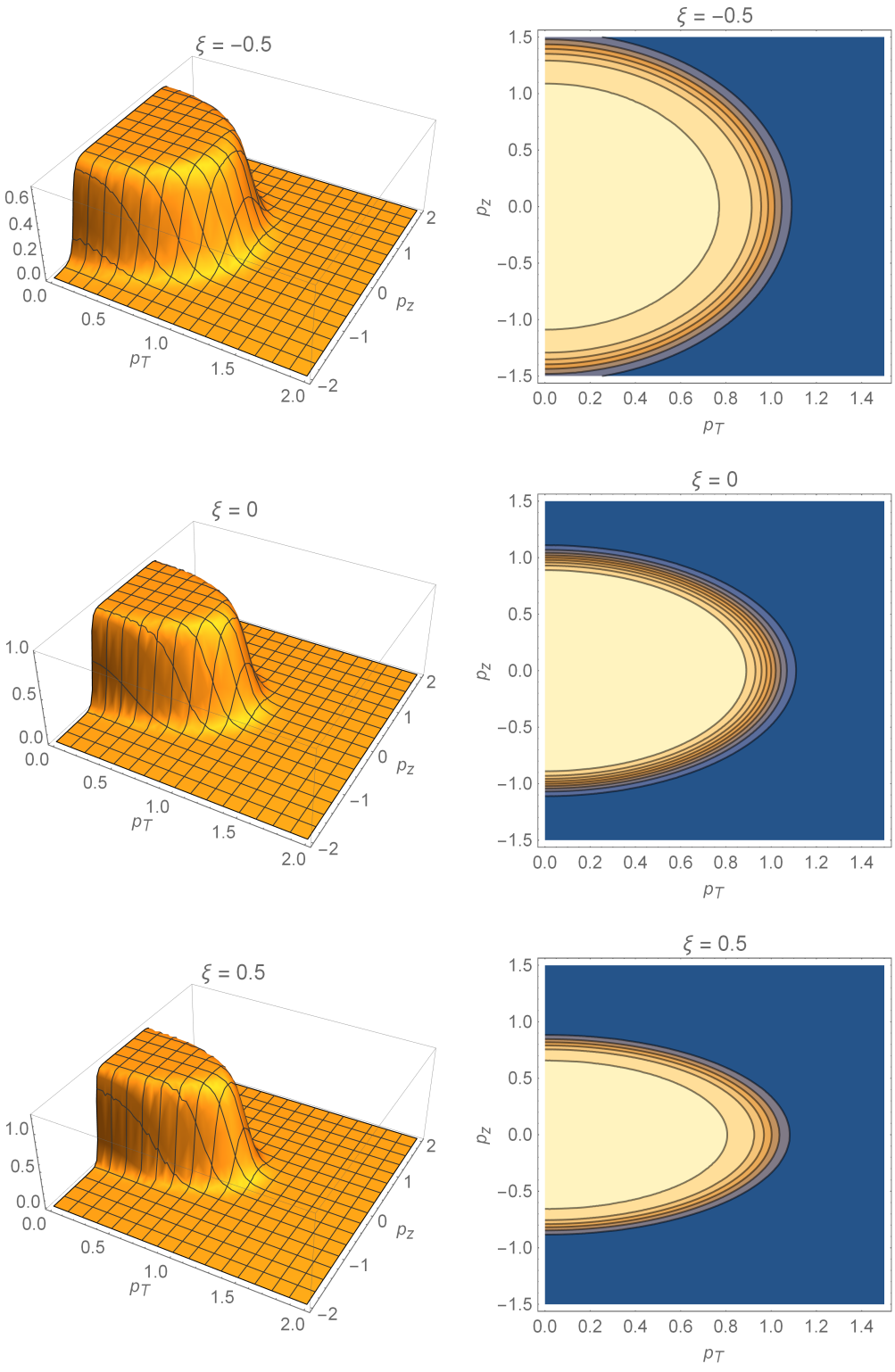

Figure 18: 3D and contour plots of an anisotropized Fermi-Dirac distribution for various values of ξ

boost parameter b which introduces a net flow in the z direction. This can be interpreted as a boost out of the rest frame.

We are therefore interested in the family of initial conditions

$$f(\omega, p_z) = \left(\sqrt{1+\xi}\right) \frac{f_0}{e^{\frac{1}{T}\left(\sqrt{\omega^2+\xi p_z^2}+bp_z-Q\right)}+1}. \tag{176}$$

(As before, for implementation purposes we multiply by an overall factor of $e^{-0.01\omega}$)

We illustrate the evolution of an underpopulated initial condition of the form of (176) with $f_0 = 0.1$, $T = 0.05$, $\xi = b = 0.2$, and $Q = 1$.

Recall that the distribution function is parameterized by B-lines, each corresponding to an individual cell. Rather than plotting the evolution of the distribution function directly (a challenge to portray on a single set of axes in 3D), we plot in Figs. 19-21 the evolution of the u, T and μ parameters in the various cells, showing convergence to a single equilibrium value for each.

As before, we are interested in the equilibriation time, which we measure by tracking the entropy, normalized by the entropy of the final equilibrium distribution. In particular we would like to compare it to the time taken for the initially anisotropic distribution function to isotropize.

To this end, as a measure of the anisotropy of a distribution function, we define the "anisotropy parameter"

$$\alpha = \frac{T^{22}_{LRF}}{T^{33}_{LRF}}, \tag{177}$$

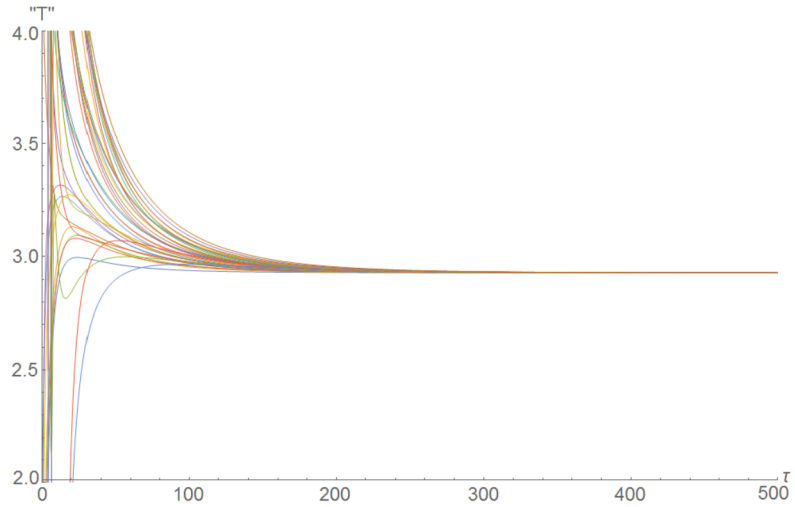

Figure 19: Evolution of the T parameter in each cell

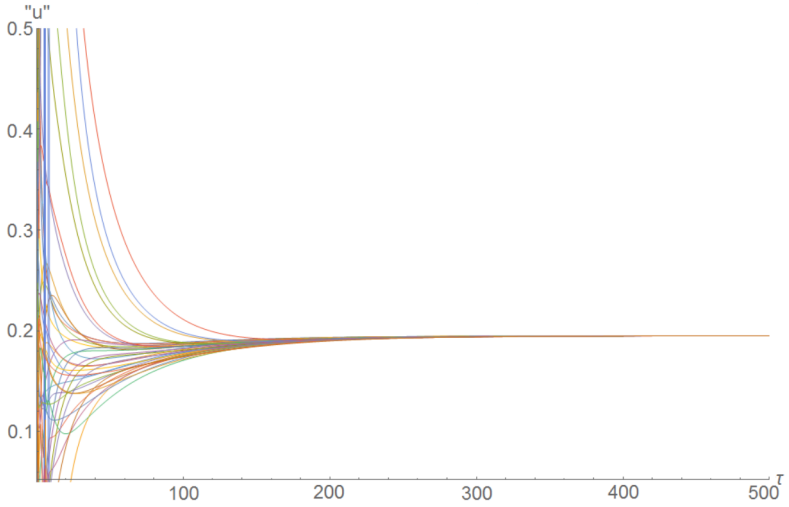

Figure 20: Evolution of the u parameter in each cell

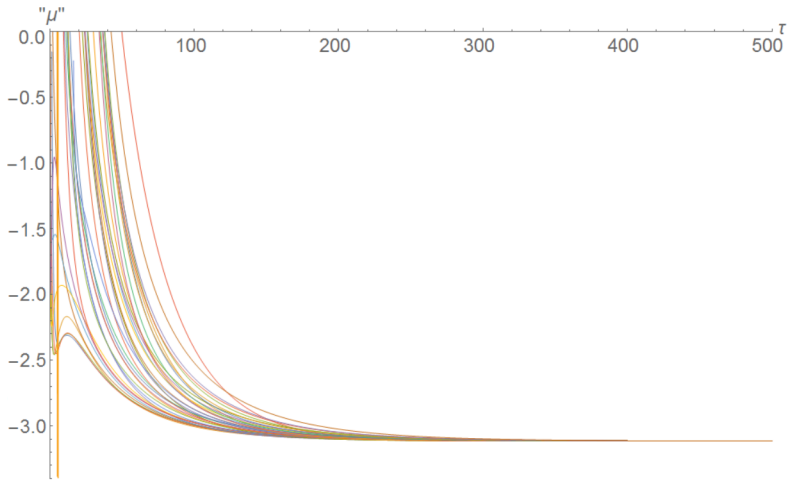

Figure 21: Evolution of the local μ parameter in each cell

where $T^{\mu\nu}_{LRF}$ is the energy-momentum tensor in the local rest frame. In the rest frame, for a cylindrically symmetric distribution function with some anisotropy, $T^{11} = T^{22} = P_\perp$ is the transverse pressure of the fluid, while $T^{33} = P_z$ is the longitudinal pressure. For an isotropic distribution they are equal; thus the ratio must also approach 1 as the system isotropizes.

We can plot the normalized entropy and the anisotropy parameter alongside each other to compare their evolution by eye.

Plotting $\ln(1 - \frac{S}{S_\infty})$ and $\ln(\alpha - 1)$ instead, we can fit straight lines to the linear portions of the evolution.

From the fit, the gradients of the lines are -0.0178 and -0.0177 - which suggests that the rates of isotropization and equilibriation are correlated.

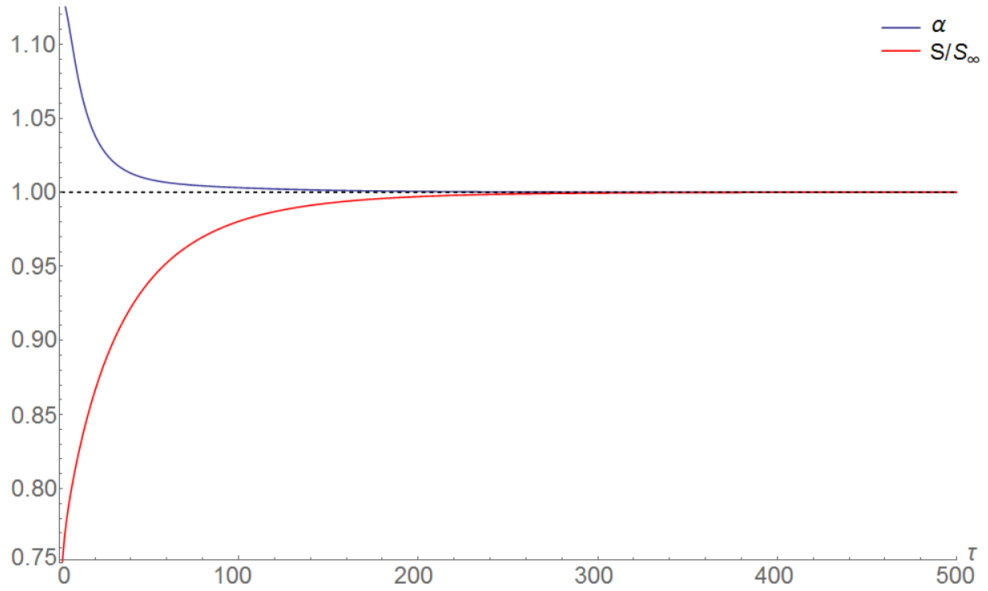

Figure 22: Evolution of the normalized entropy (Eq. (171)), and anisotropy parameter (Eq. (177))

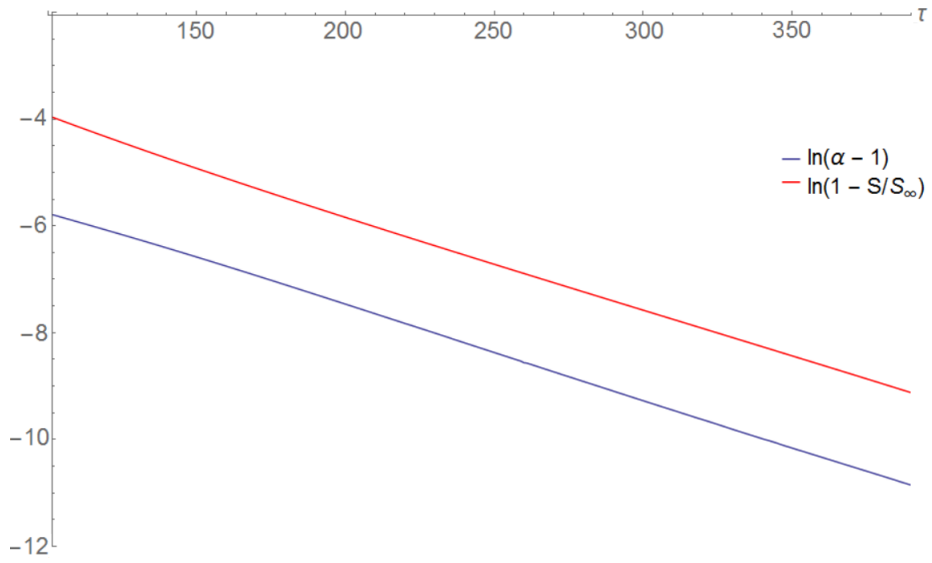

Figure 23: Linearized evolution of the normalized entropy and anisotropy parameters

6 Summary and Outlook

In this thesis we have developed a numerical scheme to solve the relativistic Boltzmann equation for gluons in the small-scattering approximation under the assumption of cylindrically symmetric initial conditions and spatial homogeneity. Among our results, we have presented an argument for the formation of a transient Bose-Einstein condensate state for certain initial conditions. We have investigated the rate at which an anisotropic distribution function becomes isotropic and compared it to the rate of thermalization. Further, we have compared these results to the relaxation time approximation to the Boltzmann equation and estimated the appropriate value of the relaxation time parameter from the small-scattering angle scheme.

Scope for further extension of this scheme exists, and such an extension is planned. In particular, it is desirable to extend the scheme to handle fully general initial conditions. We briefly present an outline of how this might be implemented.

For a general system with three degrees of freedom in momentum space, a staggered cubic grid could be employed. In such a grid, the basic unit of the interpolation would be an irregular tetrahedron (it is unfortunately impossible to tile $\mathbb{R}^3$ with regular tetrahedra). One possible arrangement would be the so-called "marching tetrahedra" (See figure 24).

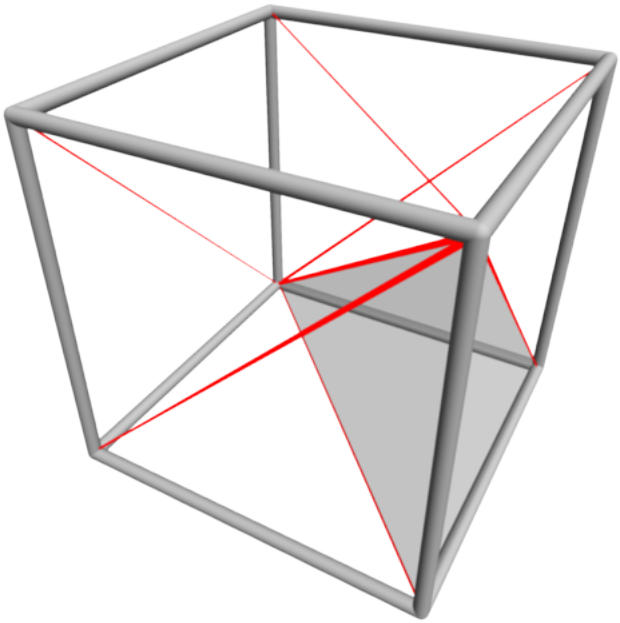

Figure 24: Cube tiled by marching tetrahedra, with one tetrahedron shaded.

The particle current in the general case is calculated in the appendices.

The final goal would be to remove the assumption of spatial homogeneity and describe a 3+3 dimensional system in which the above scheme would essentially represent a single spatial cell. Of concern is the fact that the computational complexity scales geometrically with each additional degree of freedom. (Boltzmann equation solvers typically rely on assumptions of symmetry, and for good reason). This "curse of dimensionality" would represent a significant challenge to overcome.

7 Appendices

7.1 The Polylogarithm Function

The polylogarithm of order s, $\mathrm{Li}_s(z)$, is a special function that appears inter alia in the closed forms of integrals of the Fermi-Dirac and Bose-Einstein distributions.

The function can be defined by the infinite series

$$\mathrm{Li}_s(z) = \sum_{k=1}^{\infty} \frac{z^k}{k^s} = z + \frac{z^2}{2^s} + \frac{z^3}{3^s} + ... \tag{178}$$

which is valid for arbitrary complex order s and complex arguments z with $|z| < 1$. It can be extended to arguments $|z| \geq 1$ via analytic continuation.

The name of the polylogarithm comes from the fact that it can also be defined recursively as the repeated integral of itself,

$$\mathrm{Li}_{s+1}(z) = \int_0^z \frac{dt}{t} \mathrm{Li}_s(t), \tag{179}$$

where $\mathrm{Li}_1(z) = -\ln(1-z)$ is related to the natural logarithm. The integral of the natural logarithm therefore yields the polylogarithm of order 2 (or "dilogarithm"), the integral of the dilogarithm yields the trilogarithm and so on.

A useful identity for polylogarithms of integer order relates them to the Bernoulli polynomials,

$$\begin{aligned}
\mathrm{Li}_n(z) + (-1)^n \mathrm{Li}_n(1/z) &= -\frac{(2\pi i)^n}{n!} B_n \left(\frac{1}{2} + \frac{\ln(-z)}{2\pi i} \right) \quad (z \notin (0;1]), \\
\mathrm{Li}_n(z) + (-1)^n \mathrm{Li}_n(1/z) &= -\frac{(2\pi i)^n}{n!} B_n \left(\frac{1}{2} - \frac{\ln(-1/z)}{2\pi i} \right) \quad (z \notin (1;\infty)),
\end{aligned} \tag{180}$$

where both expressions agree for $z < 0$. For implementation purposes (particularly in Mathematica) it is frequently convenient to use this to replace polylogarithms in expressions with manifest imaginary components.

7.2 Derivation of the current in the general case

In section 3.3 we generalize the particle current $\mathcal{J}(\boldsymbol{p})$ from spherically to cylindrically symmetric distribution functions. Here we present a derivation of the current for a distribution function with the full 3 degrees of freedom in momentum space.

Recall expression (101) for the current,

$$\mathcal{J}_i(\boldsymbol{p}) = C f_p \bar{f}_p \int \mathcal{V}_{ij} \nabla_k^j f_k - C \nabla_p^j f_p \int \mathcal{V}_{ij} f_k \bar{f}_k. \tag{181}$$

Where as in the cylindrical case the two integrals correspond to a vector quantity $J_i \equiv \int \mathcal{V}_{ij} \nabla_k^j f_k$ and a tensor quantity $\mathbb{J}_{ij} = \int \mathcal{V}_{ij} f_k \bar{f}_k$, each being a functional of the distribution function f.

The current (181) is defined for a specific momentum $\boldsymbol{p}$. For this $\boldsymbol{p}$ we then integrate over all possible values of $\boldsymbol{k}$.

We can represent the $\mathcal{V}_{ij}$ tensor (89) as a matrix,

$$\mathcal{V}_{ij} = \begin{pmatrix} 1 + v_x w_x - v_y w_y - v_z w_z & v_y w_x + v_x w_y & v_z w_x + v_x w_z \\ v_y w_x + v_x w_y & 1 - v_x w_x + v_y w_y - v_z w_z & v_z w_y + v_y w_z \\ v_z w_x + v_x w_z & v_z w_y + v_y w_z & 1 - v_x w_x - v_y w_y + v_z w_z \end{pmatrix}. \tag{182}$$

Thus we find for the components of the first integral in (181),

$$\begin{aligned} \mathcal{V}_{1j}\nabla_k^j f_k &= \begin{pmatrix} 1 + v_x w_x - v_y w_y - v_z w_z, & v_y w_x + v_x w_y, & v_z w_x + v_x w_z \end{pmatrix} \begin{pmatrix} \frac{\partial f_k}{\partial k_x} \\ \frac{\partial f_k}{\partial k_y} \\ \frac{\partial f_k}{\partial k_z} \end{pmatrix} \\ &= (1 + v_x w_x - v_y w_y - v_z w_z)\frac{\partial f_k}{\partial k_x} + (v_y w_x + v_x w_y)\frac{\partial f_k}{\partial k_y} + (v_z w_x + v_x w_z)\frac{\partial f_k}{\partial k_z}, \\ \mathcal{V}_{2j}\nabla_k^j f_k &= \begin{pmatrix} v_y w_x + v_x w_y, & 1 - v_x w_x + v_y w_y - v_z w_z, & v_z w_y + v_y w_z \end{pmatrix} \begin{pmatrix} \frac{\partial f_k}{\partial k_x} \\ \frac{\partial f_k}{\partial k_y} \\ \frac{\partial f_k}{\partial k_z} \end{pmatrix} \\ &= (v_y w_x + v_x w_y)\frac{\partial f_k}{\partial k_x} + (1 - v_x w_x + v_y w_y - v_z w_z)\frac{\partial f_k}{\partial k_y} + (v_z w_y + v_y w_z)\frac{\partial f_k}{\partial k_z}, \\ \mathcal{V}_{3j}\nabla_k^j f_k &= \begin{pmatrix} v_z w_x + v_x w_z, & v_z w_y + v_y w_z, & 1 - v_x w_x - v_y w_y + v_z w_z \end{pmatrix} \begin{pmatrix} \frac{\partial f_k}{\partial k_x} \\ \frac{\partial f_k}{\partial k_y} \\ \frac{\partial f_k}{\partial k_z} \end{pmatrix} \\ &= (v_z w_x + v_x w_z)\frac{\partial f_k}{\partial k_x} + (v_z w_y + v_y w_z)\frac{\partial f_k}{\partial k_y} + (1 - v_x w_x - v_y w_y + v_z w_z)\frac{\partial f_k}{\partial k_z}. \end{aligned} \tag{183}$$

Note that $\int_{-\infty}^{\infty} dk_i \frac{\partial f_k}{\partial k_i} = f_k|_{-\infty}^{\infty} = 0$ since the distribution function vanishes for large momenta. Thus only terms of $\int \frac{k_i}{k}\frac{\partial f_k}{\partial k_i}$ survive. Integrating by parts we have

$$\begin{aligned}\int_{-\infty}^{\infty} dk_x \frac{k_x}{\sqrt{k_x^2+k_y^2+k_z^2}} \frac{\partial f_k}{\partial k_x} &= \frac{k_x}{k} f_k|_{-\infty}^{\infty} - \int_{-\infty}^{\infty} dk_x \left(-\frac{k_x^2}{k^3} + \frac{1}{k}\right) f_k \\ &= \int_{-\infty}^{\infty} dk_x \left(\frac{k_x^2}{k^3} - \frac{1}{k}\right) f_k,\end{aligned} \tag{184}$$

with corresponding expressions for k_y and k_z.

Altogether, the non-vanishing terms of J_x are

$$\begin{aligned}J_x &= w_x \int v_x \frac{\partial f_k}{\partial k_x} + v_y \frac{\partial f_k}{\partial k_y} + v_z \frac{\partial f_k}{\partial k_z} \\ &= w_x \int \left(\frac{k_x^2+k_y^2+k_z^2}{k^3} - \frac{3}{k}\right) f_k \\ &= -w_x \int \frac{2}{k} f_k.\end{aligned} \tag{185}$$

Similarly

$$\begin{aligned}J_y &= -w_y \int \frac{2}{k} f_k, \\ J_z &= -w_z \int \frac{2}{k} f_k.\end{aligned} \tag{186}$$

Defining

$$I_b \equiv \int \frac{2}{k} f_k, \tag{187}$$

we can simply write

$$\mathcal{J} = \frac{\boldsymbol{p}}{p} I_b. \tag{188}$$

Now consider the tensor term $\mathbb{J}_{ij}$ in (181). Expanding $\mathbb{J}_{ij}\nabla_p^j f_p$ we have

$$\begin{aligned}\mathbb{J}_{1j}\nabla_p^j f_p &= \int \begin{pmatrix} 1 + v_x w_x - v_y w_y - v_z w_z, & v_y w_x + v_x w_y, & v_z w_x + v_x w_z \end{pmatrix} \begin{pmatrix} \frac{\partial f_p}{\partial p_x} \\ \frac{\partial f_p}{\partial p_y} \\ \frac{\partial f_p}{\partial p_z} \end{pmatrix} f_k \bar{f}_k \\ &= \frac{\partial f_p}{\partial p_x} \int (1 + v_x w_x - v_y w_y - v_z w_z) f_k \bar{f}_k + \frac{\partial f_p}{\partial p_y} \int (v_y w_x + v_x w_y) f_k \bar{f}_k \\ &\quad + \frac{\partial f_p}{\partial p_z} \int (v_z w_x + v_x w_z) f_k \bar{f}_k. \end{aligned} \tag{189}$$

We can tidy this expression by defining

$$\begin{aligned} I_a &\equiv \int f_k \bar{f}_k, \\ \mathcal{I}_i &\equiv \int v_i f_k \bar{f}_k, \end{aligned} \tag{190}$$

and writing $w_i = p_i/p$. As it is no longer necessary to differentiate between f_p and f_k, we drop the subscript. Then

$$\begin{aligned}\mathbb{J}_{1j}\nabla_p^j f_p &= \frac{\partial f_p}{\partial p_x}\left(I_a + \frac{p_x}{p}\mathcal{I}_x - \frac{p_y}{p}\mathcal{I}_y - \frac{p_z}{p}\mathcal{I}_z\right) + \frac{\partial f_p}{\partial p_y}\left(\frac{p_x}{p}\mathcal{I}_y + \frac{p_y}{p}\mathcal{I}_x\right) \\ &+ \frac{\partial f_p}{\partial p_z}\left(\frac{p_z}{p}\mathcal{I}_x + \frac{p_x}{p}\mathcal{I}_z\right) \\ &= \frac{\partial f_p}{\partial p_x}I_a + \left(\frac{p_x}{p}\frac{\partial f_p}{\partial p_x} + \frac{p_y}{p}\frac{\partial f_p}{\partial p_y} + \frac{p_z}{p}\frac{\partial f_p}{\partial p_z}\right)\mathcal{I}_x + \left(\frac{p_x}{p}\frac{\partial f_p}{\partial p_y} - \frac{p_y}{p}\frac{\partial f_p}{\partial p_x}\right)\mathcal{I}_y \\ &+ \left(\frac{p_x}{p}\frac{\partial f_p}{\partial p_z} - \frac{p_z}{p}\frac{\partial f_p}{\partial p_x}\right)\mathcal{I}_z,\end{aligned} \tag{191}$$

and similarly

$$\begin{aligned}\mathbb{J}_{2j}\nabla_p^j f_p &= \frac{\partial f_p}{\partial p_y}I_a + \left(\frac{p_y}{p}\frac{\partial f_p}{\partial p_x} - \frac{p_x}{p}\frac{\partial f_p}{\partial p_y}\right)\mathcal{I}_x + \left(\frac{p_x}{p}\frac{\partial f_p}{\partial p_x} + \frac{p_y}{p}\frac{\partial f_p}{\partial p_y} + \frac{p_z}{p}\frac{\partial f_p}{\partial p_z}\right)\mathcal{I}_y \\ &+ \left(\frac{p_y}{p}\frac{\partial f_p}{\partial p_z} - \frac{p_z}{p}\frac{\partial f_p}{\partial p_y}\right)\mathcal{I}_z,\end{aligned} \tag{192}$$

and

$$\begin{aligned}\mathbb{J}_{3j}\nabla_p^j f_p &= \frac{\partial f_p}{\partial p_z}I_a + \left(\frac{p_z}{p}\frac{\partial f_p}{\partial p_x} - \frac{p_x}{p}\frac{\partial f_p}{\partial p_z}\right)\mathcal{I}_x + \left(\frac{p_z}{p}\frac{\partial f_p}{\partial p_y} - \frac{p_y}{p}\frac{\partial f_p}{\partial p_z}\right)\mathcal{I}_y \\ &+ \left(\frac{p_x}{p}\frac{\partial f_p}{\partial p_x} + \frac{p_y}{p}\frac{\partial f_p}{\partial p_y} + \frac{p_z}{p}\frac{\partial f_p}{\partial p_z}\right)\mathcal{I}_z.\end{aligned} \tag{193}$$

We can write down a vector expression for $\mathbb{J}_{ij}\nabla_p^j f_p$ by inspection as $I_a\boldsymbol{\nabla} f + (\boldsymbol{\nabla} f \cdot \hat{\boldsymbol{p}})\boldsymbol{\mathcal{I}} + (\boldsymbol{\nabla} f \times \hat{\boldsymbol{p}}) \times \boldsymbol{\mathcal{I}}$.

Altogether we have the complete expression for the current

$$\mathcal{J}(\boldsymbol{p}) = I_a \boldsymbol{\nabla} f + I_b f \bar{f} \hat{\boldsymbol{p}} + (\boldsymbol{\nabla} f \cdot \hat{\boldsymbol{p}}) \boldsymbol{\mathcal{I}} + (\boldsymbol{\nabla} f \times \hat{\boldsymbol{p}}) \times \boldsymbol{\mathcal{I}}. \tag{194}$$

Observing that $\mathcal{I}_i = \int v_i f \bar{f}$ vanishes for distribution functions symmetric about the i-axis, it is easy to verify that this expression reduces to the previous ones for the cases of spherical and cylindrical symmetry - (90) and (124) respectively.

References

[1] J. P. Blaizot, J. Liao, and L. McLerran. Gluon transport equation in the small angle approximation and the onset of Bose-Einstein condensation. *Nuclear Physics A*, 920:58, 2013.

[2] F. Gelis. The early stages of a high energy heavy ion collision. In *Journal of Physics Conference Series*, volume 381 of *Journal of Physics Conference Series*, page 012021, 2012.

[3] https://inspirehep.net/record/930986/plots.

[4] H. Weigert. Evolution at small x(bj): The Color glass condensate. *Prog. Part. Nucl. Phys.*, 55:461, 2005.

[5] C. C. Bradley, C. A. Sackett, J. J. Tollett, and R. G. Hulet. Evidence of Bose-Einstein Condensation in an Atomic Gas with Attractive Interactions. *Physical Review Letters*, 75:1687, 1995.

[6] L. P. Csernai and D. Strottman. *Relativistic Heavy Ion Physics, International Review of Nuclear Physics Vol 5-6*. World Scientific, 1991.

[7] S. R. de Groot, W. A. van Leeuwen, and C. G. van Weert. *Relativistic Kinetic Theory*. North-Holland, 1980.

[8] L. D. Landau and E. M. Lifshitz. *The Classical Theory of Fields*. Course of theoretical physics Vol 2. Butterworth-Heinemann, 1975.

[9] R. Hakim. *Introduction to relativistic statistical mechanics: classical and quantum*. World scientific, Singapore, 2011.

[10] C. Eckart. The Thermodynamics of Irreversible Processes. III. Relativistic Theory of the Simple Fluid. *Phys. Rev.*, 58:919, 1940.

[11] F. Schwabl and W. D. Brewer. *Statistical Mechanics*. Advanced Texts in Physics. Springer Berlin Heidelberg, 2006.

[12] L. D. Landau and E. M. Lifshitz. *Mechanics*. Butterworth-Heinemann, 1976.

[13] E. A. Uehling and G. E. Uhlenbeck. Transport Phenomena in Einstein-Bose and Fermi-Dirac Gases. I. *Physical Review*, 43:552, 1933.

[14] M. E. Peskin and D. V. Schroeder. *An Introduction to Quantum Field Theory; 1995 ed.* Westview, 1995.

[15] W. Florkowski. *Phenomenology of Ultra-Relativistic Heavy-Ion Collisions*. World Scientific, 2010.

[16] L. Rezzolla and O. Zanotti. *Relativistic Hydrodynamics*. OUP Oxford, 2013.

[17] C. Cercignani and G. M. Kremer. *The Relativistic Boltzmann Equation: Theory and Applications*. Birkhäuser Basel, 2002.

[18] Kai Zhou, Zhe Xu, Pengfei Zhuang, and Carsten Greiner. Kinetic description of Bose-Einstein condensation with test particle simulations. *Phys. Rev.*, D96(1):014020, 2017.

[19] A. Peshier, B Kämpfer, O. P. Pavlenko, and G. Soff. A Massive quasiparticle model of the SU(3) gluon plasma. *Phys. Rev. D*, 54:2399, 1996.

[20] A. D. Fokker. Die mittlere Energie rotierender elektrischer Dipole im Strahlungsfeld. *Annalen der Physik*, 348(5):810, 1914.

[21] M. Planck. *Über einen Satz der statistischen Dynamik und seine Erweiterung in der Quantentheorie.* Sitzungsberichte der Königlich-Preussischen Akademie der Wissenschaften zu Berlin. 1917.

[22] W. E. Schiesser. *The Numerical Method of Lines: Integration of Partial Differential Equations.* Academic Press, 1991.

[23] J. L. Anderson and H. R. Witting. A relativistic relaxation-time model for the Boltzmann equation. *Physica*, 74:466, 1974.

[24] B. Schenke and M. Strickland. Fermionic Collective Modes of an Anisotropic Quark-Gluon Plasma. *Phys. Rev. D*, 74:065004, 2006.